

**ANGULAR MOMENTUM EXCHANGE AMONG THE SOLID EARTH,
ATMOSPHERE AND OCEANS:
A CASE STUDY OF THE 1982-83 EL NIÑO EVENT**

by

J. O. Dickey¹, S. L. Marcus¹, R. Hide^{2,1}, T. M. Eubanks³ and D. H. Boggs¹

¹Space Geodetic Science and Applications Group
Jet Propulsion Laboratory
California Institute of Technology
Pasadena, California 91109-8099 USA

²Oceanography Group, Clarendon Laboratory
The Observatory, Parks Road
Oxford OX1 3PU, England, U.K.

³U.S. Naval Observatory
Washington, D. C. 20392-5420

J. Geophys. Res. (submitted)

January 3, 1994

Outline

Abstract

1. Introduction
2. Data Considered
 - 2.1 Length-of-day
 - 2.2 Atmospheric Angular Momentum
 - 2.3 Southern Oscillation Index
3. Atmospheric Excitation of Interannual Variations
 - 3.1 Background
 - 3.2 Stratospheric Contribution
 - 3.3 Bimodality Analysis
 - 3.4 Error Estimates
4. Role of the Oceans
5. Summary

Acknowledgments

Appendix

References

Tables

Figure Captions

Figures

ABSTRACT

The 1982-83 El Niño/Southern Oscillation (ENSO) event was accompanied by the largest interannual variation in the Earth's rotation rate on record. In this study we demonstrate that **atmospheric forcing** was the dominant cause for this **rotational anomaly**, with **atmospheric angular momentum (AAM)** integrated from 1000 to 1 mb (troposphere plus atmosphere) accounting for up to 92% of the interannual variance in the length-of-day (LOD). Winds between 100 and 1 mb contributed nearly 20% of the variance explained, indicating that the stratosphere can play a significant role in the Earth's angular momentum budget on interannual time scales. Examination of LOD, AAM, and Southern Oscillation Index (SOI) data for a 15-year span surrounding the 1982-83 event suggests that the strong rotational response resulted from constructive interference between the low-frequency (~ 4-6 year) and quasi-biennial (~ 2-3 year) components of the ENSO phenomenon, as well as the stratospheric QBO. Sources of the remaining LOD discrepancy (~ 55 μ s) are explored; data noise and systematic errors are estimated to contribute 18 and 33 μ s, respectively, leaving a residual of 40 μ s unaccounted for. Oceanic angular momentum contributions (both moment of inertia changes associated with baroclinic waves and motion terms) are shown to be candidates in closing the interannual axial angular momentum budget.

1. Introduction

The rotation rate of the solid Earth exhibits minute but complicated changes of up to several parts in 10^8 in speed [corresponding to a variation of several milliseconds in the length of day (LOD)] and even larger variations in the direction of the rotation axis (polar motion). These changes occur over a broad spectrum of time scales, ranging from days to centuries and longer, reflecting the fact that they are produced by a wide variety of geophysical and astronomical phenomena. The extent to which fluctuations in the angular momentum of the atmosphere $H_i(t)$ give rise to compensating changes in the angular

momentum of the solid Earth, thereby exciting contributions to LOD [$\equiv \Lambda(t)$], has been the subject of many studies. Advances have been made possible by the availability for the past decade of routine daily or twice-daily determinations of all three components of $H_i(t)$ by several meteorological agencies [see for example, *Hide and Dickey*, 1991 and references therein]. These studies are facilitated by the use of dimensionless functions χ_i , $i = 1, 2, 3$ introduced by *Barnes et al.* [1983] related to the equatorial components H_1 and H_2 , and the axial component H_3 .

The axial component χ_3 satisfies

$$\chi_3 \equiv \frac{R^3}{gC_m\Omega_0} \int_0^{P_s} \int_{-\pi/2}^{\pi/2} \int_0^{2\pi} u \cos^2 \phi \, d\lambda \, d\phi \, dp + \frac{0.70R^4}{gC_m} \int_{-\pi/2}^{\pi/2} \int_0^{2\pi} p_s \cos^3 \phi \, d\lambda \, d\phi \quad (1.1)$$

where (ϕ, λ) denote latitude and longitude respectively, $p_s(\phi, \lambda, t)$ is the surface pressure and $u(\phi, \lambda, p, t)$ the eastward (westerly) component of the wind velocity at the pressure level p . The calculations presented here follow *Barnes et al.* [1983] and take $R = 6.37 \times 10^6$ m for the mean radius of the solid Earth, and $g = 9.81 \text{ ms}^{-2}$ for the mean acceleration due to gravity. The coefficient 0.70 incorporates the so-called ‘‘Love number’’ correction which allows for small concomitant changes in the inertia tensor of the imperfectly-rigid solid Earth. The dominant contribution to fluctuations in $\chi(t)$ comes from the ‘‘wind’’ term given by the first integral of the right-hand side of equation (1.1), which depends on the strength of the zonally averaged eastward wind speed u and also on its distribution with latitude. Fluctuations in the ‘‘matter’’ term given by the second integral are generally smaller, but make a significant contribution.

The seasonal and intraseasonal LOD components are well accounted for in terms of the exchange of angular momentum between the atmosphere and the solid Earth [see for example *Lambeck*, 1988; *Hide and Dickey*, 1991 and references therein]. Meteorological effects cannot be the dominant cause of the larger decadal variations, but it is a matter for investigation as to whether meteorological excitation is the main cause of the interannual

variations on time scales ranging from 1 to 5 years. The amplitude of this component of the spectrum, up to 0.5 ms, is comparable with that of the seasonal cycle (see Fig. 1), implying that the atmosphere could play a significant role in its generation.

Fig. 1 near here

In this paper we adduce evidence that atmospheric motions are largely responsible for generating Earth rotation fluctuations on these interannual time scales, focusing on the 1982-83 ENSO event. These results are obtained from comparisons of the interannual LOD fluctuations with operational atmospheric angular momentum (AAM) estimates, combined with geostrophic wind estimates derived from satellite temperature soundings of the stratosphere. A description of the data sets is presented in Section 2. Sections 3 and 4 deal with the atmospheric and oceanic excitation of interannual LOD variations, respectively. Results are summarized in the final section. The reader is also referred to several more general accounts of the excitation of Earth orientation changes. References to early work can be found in the classical monograph on the subject by *Munk and MacDonald*, [1960] and to more recent work in various monographs and other publications [e.g., *Cazenave*, 1986; *Dickey*, 1993; *Dickey and Eubanks*, 1986; *Eubanks*, 1993; *Hide*, 1977, 1984, 1986; *Hide and Dickey*, 1991; *Lambeck*, 1980 and 1988; *Moritz and Mueller*, 1987; *Rosen*, 1993; and *Wahr*, 1988].

2. Data Considered

2.1 Length-of-Day

The LOD series utilized (Fig. 1) is the Jet Propulsion Laboratory (JPL) Kalman-filtered series, which combines Earth rotation results from optimal astrometry, Very Long Baseline Interferometry (VLBI) and Lunar Laser Ranging (LLR) to form a high-quality series, in which the issues of reference frame commonality and the unevenness of data quality and quantity have been addressed [*Gross*, 1992; *Morabito et al.*, 1988]. The LOD data improves in quality with time, especially after 1985. In 1976 the uncertainty is about

0.09 ms, decreasing almost linearly to about 0.03 ms in 1985 and thereafter. During the 1982-83 ENSO, the uncertainty is 0.05-0.06 ms. Since the average spacing of data points used as input to the Kalman filter at this time is about five days, we estimate that annual mean LOD values during the 1982-83 ENSO contain ~ 73 degree of freedom, so that the error associated with interannual variations is $\sim 7 \mu\text{s}$ [see *Dickey et al.*, 1992a for a further discussion of the spectral characteristics of LOD errors].

2.2 Atmospheric Angular Momentum

For the AAM data, we use two series that are available during the 1982-83 ENSO event, from the National Meteorological Center (NMC) and the European Centre for Medium Range Weather Forecasts [ECMWF—see *Salstein et al.*, 1993 for a review of existing data]. Analyses incorporating winds up to the 100 and 50 mb levels, respectively, as well as the full pressure term are available from both centers; in addition, the pressure term incorporating the inverted barometer correction is provided by the NMC. We also consider zonal wind variations from 100 mb to the 1 mb level, computed by *Hirota* [1983] from temperature soundings using the geostrophic assumptions [see *Rosen et al.*, 1985 for further details of this series]. These data were combined with the 100 mb values to obtain AAM variations incorporating almost the full atmosphere (1000 to 1 mb). Formal errors are not provided with the AAM values; estimates of the uncertainty in the AAM data are considered in Section. 3.4

2.3 Southern Oscillation Index

We use here a modified version of the index based on the Tahiti and Darwin surface pressure data, provided by the NMC Climate Analysis Center [*Rasmusson*, private communication]. Our “Modified Southern Oscillation Index” (MSOI) is given as the difference between the Darwin and Tahiti surface pressures in millibars, and is positively correlated with the LOD.

3. Atmospheric Excitation of Interannual LOD Variation

3.1 Background

Several earlier studies attempted to link interannual LOD variations (defined here to be Λ^*_β , following notation of Hide and Dickey, 1991—see Fig. 1) to the Quasi-Biennial Oscillation (QBO) exhibited by zonal winds in the equatorial stratosphere [for a review, see *Lambeck*, Chapter 7, 1980]. *Lambeck and Cazenave* [1973], for example, associated Λ^*_β changes during the 1955-71 period with the QBO. Subsequent work by *Stephanic* [1982] indicated a connection between Λ^*_β and the “Southern Oscillation” by establishing coherence between Λ^*_β and fluctuations in equatorial Pacific air temperature, which is related to the intensity of the Southern Oscillation. Further investigations were stimulated by the occurrence of an unusually strong and well observed El Niño in 1982-83 [see e.g. *Philander*, 1983 and 1990; *Rasmusson and Wallace*, 1983]. The largest changes ever recorded in Λ^*_β and AAM occurred during January and February 1983 [*Rosen et al.*, 1984 and *Eubanks et al.*, 1985a].

The El Niño/Southern Oscillation (ENSO) phenomenon is associated with persistent but irregular variations of atmospheric pressure over the South Pacific on interannual time scales. This gives rise to pronounced year-to-year variations in the climate of the South Pacific basin [*Rasmusson and Wallace*, 1983] associated with extensive fluctuations in the atmospheric and oceanic circulation and in sea surface temperatures [*Philander*, 1983 and 1990]. The dynamical processes involved include nonlinear air-sea interactions, with changes in the sea surface temperature causing changes in the surface winds which, in turn, modify ocean surface waters, providing a feedback loop. The persistence of the oscillation is probably a consequence of the thermal inertia of the oceans, which provides a means of storing heat from one year to the next. According to a model by *Wyrtki* [1985], the ENSO cycle is driven by the steady accumulation of warm water in the western part of the equatorial Pacific caused by the prevailing surface easterly winds. An El

Niño event is triggered by a relaxation of the easterlies, which causes a surge of warm water to move from the West to the East Pacific until it encounters the coasts of North and South America, where it is deflected to higher latitudes in both hemispheres. The El Niño events thus serve to remove the excess warm equatorial water, setting the stage for the oscillation to begin again. The associated “Southern Oscillation” in surface air pressure has the structure of a standing wave, with antinodes near the eastern and western boundaries of the South Pacific, $\sim 90^\circ$ longitude apart [Horel and Wallace, 1981]. This has led to the development of various Southern Oscillation Indices (SOI) based on the difference between sea level surface pressure in the East and West Pacific. The most commonly used index is based on the normalized seasonally adjusted pressure difference between Tahiti, in the east, and Darwin, Australia, in the west [Chen, 1982].

Figure 2 presents a comparison between interannual variations in the Earth's rotation, measured as changes in $\Lambda_\beta(t)$, and the strength of the ENSO cycle, represented by the Modified Southern Oscillation Index (MSOI—see Section 2.3) series. Here the interannual fluctuations are taken to be the difference between one-year and five-year running means of each data type. The agreement between the two series is striking, with high interannual values of LOD generally coinciding with ENSO events, represented as periods for which the MSOI has a continuous positive anomaly of more than one-half its standard deviation. During an ENSO event, the MSOI (SOI) reaches a maximum (minimum), leading to an increase in $\chi_3(t)$ associated with the collapse of the tropical easterlies. Further increases in $\chi_3(t)$ may result from a strengthening of westerly flow in the sub-tropical jet streams [Rosen *et al.*, 1984]. Conservation of total angular momentum then requires the Earth's rate of rotation to slow down, thus increasing Λ . The largest variations seen in $\Lambda_\beta(t)$ are evidently associated with the 1982-83 ENSO event.

Fig. 2 near here

A one-month time-lag in $\Lambda_\beta(t)$ relative to the MSOI is found to give the maximum cross-correlation (0.67). For shorter record lengths, higher correlations are obtained (e.g.,

a correlation of 0.79 with $\Lambda_{\beta}(t)$ lagging the MSOI by two months for the period 1972-1986), although the level of statistical significance is about the same [Dickey *et al.*, 1993]. Other studies have indicated significant correlation between interannual LOD variations and indices of the Southern Oscillation; Chao [1984] reported a correlation coefficient of 0.56 for the period 1957-1983, while Eubanks *et al.* [1986] computed a correlation coefficient of ~ 0.5 for the period 1962-1984, and Chao [1988] found a correlation of 0.68 for the period 1962-1984. Chao [1989] also obtained a correlation coefficient of 0.75 for the period 1964-1984 by using multiple regression on the SOI and a stratospheric AAM series, derived from monthly data from three stations using an *idealized* model of the QBO.

3.2 Stratospheric Contribution

Routine determinations of the atmospheric χ functions are available since 1976, using data compiled from the NMC. Figure 3 shows a comparison between LOD and AAM, calculated from zonal winds integrated up to the 100 mb level, for the 15-year period extending from June, 1976, to May, 1991. Since the LOD is given as a residual from the standard length-of-day (86400 SI seconds), the vertical offset between the LOD and AAM curves has no physical significance. Note that the quality and quantity of the space-geodetic data improved substantially in 1985, resulting in a higher time-resolution LOD series after this time. Excellent agreement is seen between the two series over the entire span when variations with periods of two years or less are considered. Considerable discrepancy is found on longer time scales, however, as indicated by the divergence of the annual running means for the two data types (dot-dash lines in Fig. 3).

Fig. 3 near here

Previous studies [Dickey *et al.*, 1990 and Rosen *et al.*, 1990] found the residual between the overlapping LOD and AAM series to be dominated by a long-term linear drift with some indication of a second-order term being significant. Examination of the residual with the longer data sets now available shows the clear presence of a second-order term

(bottom curve in Fig. 3), which is due to decadal effects present in the LOD series. Interannual changes are also seen in the slope of the residual, and have been associated with the ENSO phenomenon [Dickey *et al.*, 1990]; Rosen *et al.* [1990] concluded that either core-mantle coupling is a nonsteady phenomenon or that unmodeled oceanic processes are responsible for the intermittency of the slope. The residual also shows a strong semi-annual signature, indicative of a missing stratospheric component on seasonal time scales [Rosen and Salstein, 1985].

In order to form a more quantitative estimate of atmospheric forcing during the 1982-83 ENSO, we combined the operational atmospheric analyses available from the NMC and ECMWF with the satellite-derived stratospheric data to form daily AAM series that integrate the angular momentum of the atmosphere up to 1 mb for the period 1980 through 1986. While the span of this atmospheric data is too short to allow for a spectral study, its temporal coverage is ideally suited for a case study of the intense 1982-83 El Niño, which was associated with the largest interannual variations of LOD and AAM on record (cf. Fig. 1). In order to focus on interannual variations, all series were subject to a 365-day moving average; a cosine taper was applied to the first and last 10% of the average, in order to reduce ripple effects [Bloomfield, 1976]. Decadal effects were removed by detrending each of the smoothed series.

The resulting interannual variations of AAM and LOD are shown in Fig. 4 for a three-year period (1981.5-1984.5) surrounding the 1982-83 ENSO event. The peak-to-peak LOD variation is roughly 0.5 ms (see also curve C in Fig. 1 and the upper curve in Fig. 2), with a root-mean-square (rms) amplitude of 193 μ s (see Table 1). Meteorological data from both the NMC and EC (Figs. 4a and 4b, respectively) clearly indicate that the atmosphere is the dominant source for interannual LOD variation during this event. Consideration of the full meteorological excitation (i.e. wind plus pressure terms) using data up to 100 mb reduces the rms LOD variation from 193 μ s to 99.1 μ s in the case of the European Centre (EC), explaining 73% of the variance. When the NMC data are utilized,

the residual is decreased to 104.7 μs with 70.6% of the variance accounted for. The utilization of atmospheric data integrated to 50 mb further increases the variance explained. For the EC case, the LOD-AAM residual becomes 75.8 μs (84.6% variance explained), while for the NMC data, the residual is 89.6 μs (78.4% variance explained).

Fig. 4 near here

The utilization of the atmospheric data up to the 1 mb level decreases the residual further. The EC wind plus pressure terms now accounts for 91.9% of the variance, leaving a residual of 55 μs . The corresponding NMC data set explains 89.0% of the variance with 64 μs remaining. Thus the stratosphere does make a significant contribution to interannual AAM variation during this event, with atmospheric data integrated from 100 to 1 mb explaining nearly an additional 20% of the LOD variance. This is not surprising for stratospheric winds are typically twice as strong as tropospheric winds on average. We also note that the application of EC data consistently gives lower unexplained residuals, and that the pressure term had only a small ($\lesssim 1\%$) effect on the amount of variance explained in all cases considered. The inclusion of the pressure term with the inverted barometer correction (available from the NMC analysis only) reduces the explained variance at all three levels studied, indicating some difficulty either with the inverted barometer model, or with the quality of the pressure term estimates, on interannual time scales.

Chao [1989] noted an apparent lead of the idealized stratospheric AAM with respect to LOD of about 1 month, which is the resolving interval of the data he analyzed. A similar effect can be seen in the daily data plotted in Fig. 4, where the 100mb and 50mb AAM curves show their maximum departures during the mature phase of the 1982-83 event, while the full AAM (integrated up to 1mb) has its peak near the end of the onset phase (late 1982). This implies that the strongest variations in the stratosphere preceded both the tropospheric and LOD maxima. To examine phase relationships between interannual LOD and AAM variations, we plot in Fig. 5 the variance explained by the daily AAM data sets as a function of lag with respect to the LOD series. For AAM integrated to 100 and 50 mb the

explained variance is approximately symmetric with respect to zero, with no discernible lag or lead between the two data types. When the stratospheric data are considered with NMC analysis, however, the LOD appears to lag by about 20 days, with the AAM explaining a maximum of 90% of the interannual LOD variations. A similar analysis using EC data indicates a smaller lag for the LOD (10 days with wind plus pressure and 16 days with wind only), with the AAM explaining a maximum of 92% of the variance. If we consider the difference of 2% to be a lower bound on the uncertainty in the explained variance, *these results are consistent with a null hypothesis of zero lag between the two data types and the apparent lead is not statistically significant.*

Fig. 5 near here

3.3 Bimodality Analysis

Several studies have shown that the ENSO phenomenon is bimodal in nature, with a quasi-biennial (QB) component having periods in the 2-3 year range and a low-frequency (LF) component with periods in the 4-6 year range [Rasmussen *et al.*, 1990; Barnett, 1991; Keppenne and Ghil, 1992]. For a 15-year span surrounding the 1982-83 event, in particular, spectral analysis of both LOD and SOI data further indicates bimodality with clear peaks at periods centered at 4.2 and 2.4 years [Dickey *et al.*, 1992]. Here, we use the recursive filter of Murakami [1979] to study variations of LOD, SOI, and AAM data for the same 15-year span in the QB (18-35 month) and LF (32-88 month) bands defined by Barnett [1991]. In addition, the currently available six-year record of stratospheric AAM (spanning 1980-86) is considered.

An overview of sub-decadal variability in monthly LOD, tropospheric and stratospheric AAM, and MSOI data surrounding the 1982-83 ENSO event is given in Figs. 6a-d, where fluctuations in each series are plotted as a function of time and frequency for the period 1976-1991. The largest positive signals are clearly associated with the 1982-83 and 1986-87 El Niño events (as indicated in red), with the strong La Niña of 1988-89

appearing as a negative signal in all three data types. Bimodality on interannual time scales is evident, with enhanced variability appearing at relatively low (4-6 year) and quasi-biennial (2-3 year) frequencies. ENSO and La Niña events result when variations in both bands add constructively to produce a significant index; for example, in 1977-78, 1982-83, and 1986-87, positive signals from both bands produce significant ENSO events, while in 1988-89, negative signals from both bands result in a La Niña event. In contrast, positive QB components interfere destructively with the LF components in 1980-81 and 1984-85 with no resultant events.

Fig 6 near here, please

The strong maximum found for LOD during the 1982-83 event results from nearly equal contributions from the QB and LF bands, which both show maxima in early 1983 (Figs. 6a and 7a). The phase agreement between the two components during the 1986-87 event is not as close, with the LF component, in particular, having a smaller amplitude. As a result, the sum of the two components (solid line) shows a much stronger signature during the 1982-83 event than during 1986-87; the small LOD amplitude during the latter event may be related to a change in the decadal LOD variation which occurred at about the same time [Dickey *et al.*, 1993]. The SOI also shows excellent phase agreement between the two components during the 1982-83 event (Figs. 6b and 7b), with both having about the same amplitude. This phase agreement is also preserved during the 1986-87 event, although the QB component is somewhat smaller, resulting in a diminished total amplitude relative to the 1982-83 event. Note that the coherent behavior of the two components extends into 1988, when negative values of both added constructively to give a strong La Niña episode. Note the deep valley (indicated by dark blue in Fig. 6b) extending over the full interannual range.

The decomposition of the tropospheric AAM shows a similar structure, with LF and QB components of about the same amplitude combining to produce a large signal during the 1982-83 event, and a distinctly weaker QB component giving a diminished

amplitude for the 1986-87 event (Fig. 7c). Interannual fluctuations in tropospheric AAM are closely related to the ENSO cycle, as evidenced by the similarity of their signatures in Figs. 6b and 6c. The shorter record of stratospheric AAM (Fig. 7d) also shows phase agreement between the QB and LF components during the 1982-83 event, although this decomposition is less meaningful given the limited span of data available.

The total interannual variation (sum of the QB and LF bands) for AAM in the troposphere, stratosphere, and the full atmosphere (1000-1 mb) is shown in Fig. 7e. Note that while the stratosphere as defined in this study contains only 10% of the mass of the atmosphere, its contribution to the 1982-83 rotational anomaly is roughly half that of the troposphere. This is consistent with the results of *Chao* [1989], who used multiple regression to show that an index of stratospheric AAM, derived using monthly data from three stations with an *idealized* model of the QBO, accounted for about half the LOD variation associated with the SOI. While they have similar time scales, dynamical connections between QB variations in the troposphere and stratosphere remain elusive (e.g. Xu, 1992; Barnett, 1991; see, however, Yasunari 1989); thus, it is possible that the fortuitous coincidence in phase between these two oscillations, as shown by their AAM signatures (dotted lines in Figs. 5c and 5d), may have contributed to the unusually large amplitude of the 1982-83 ENSO.

3.4 Error Estimates

The results of the case study demonstrate that atmospheric forcing was the dominant source of interannual LOD variations during the 1982-83 ENSO event, the largest for which detailed records exist. The atmosphere integrated to the 1-mb level accounted for up to 92% of the variance, leaving an unexplained rms residual of $\sim 60 \mu\text{s}$ ($55 \mu\text{s}$ and $64 \mu\text{s}$ in the EC and NMC case, respectively) in the interannual LOD. In order to investigate the source of this discrepancy, we assume that both the LOD and AAM data sets are

composed of a common geophysical signal, S , and noise components, N_L and N_A respectively, assumed to be uncorrelated with the signal and with each other:

$$\text{LOD} = L(t) = S + N_L$$

$$\text{AAM} = X(t) = S + N_A.$$

The expected power of the residual between the two series is then

$$\langle (L-X)^2 \rangle = \langle N_L^2 \rangle + \langle N_A^2 \rangle.$$

As indicated in Sect. 2.1, the estimated error pertaining to interannual LOD determinations during the period of the case study is $\sim 7 \mu\text{s}$; for a residual with rms value $\sim 60 \mu\text{s}$, therefore, the effect of the LOD error is essentially negligible ($< 1 \mu\text{s}$). Similarly, since the contribution of the atmosphere above 1 mb is estimated to be $\sim 4 \mu\text{s}$ (see Sect. 2.2), its effect on the size of the rms residual can also be neglected. We hypothesize, therefore, that the observed residual arises from noise in the AAM signal considered (1000 – 1 mb).

In order to estimate the noise associated with the AAM signal, we initially assume that AAM errors from different centers are independent. Hence, the expected power of the intercenter difference (i, j) is

$$\langle (X_i - X_j)^2 \rangle = \langle N_i^2 \rangle + \langle N_j^2 \rangle = 2 E$$

where E denotes the average squared error for the centers considered.

The rms residual between the EC and NMC (wind plus pressure) data sets at 100 mb and 50 mb is $13.1 \mu\text{s}$ and $18.2 \mu\text{s}$, respectively; hence

$$E_{1000-100} = (13.1)^2/2 = 85.5 \mu\text{s}^2$$

and

$$E_{1000-50} = (18.2)^2/2 = 165.5 \mu\text{s}^2$$

where the subscript on the left-hand side indicates the pressure levels considered. If the errors from different levels are uncorrelated, then

$$E_{100-50} = E_{1000-50} - E_{1000-100} \sim 80 \mu\text{s}^2,$$

so that the error variance of the 50-mb layer lying directly above the 100-mb level is approximately equal to that of the entire atmosphere beneath it. Since independent

determinations of stratospheric AAM were not available for the period of this study, the error for the 50–1-mb layer cannot be estimated directly. Particularly in view of the fact that winds in this layer were estimated solely from satellite temperature soundings in contrast to the operational analyses available up to the 50 mb level, it is reasonable to expect that the error variance contributed by this layer is also comparable to that of the atmosphere below it. We assume, therefore, that

$$E_{50-1} \sim E_{1000-50},$$

so that

$$E_{1000-1} = E_{50-1} + E_{1000-50} \sim 2 E_{1000-50} = 331 \mu\text{s}^2,$$

and we estimate for the AAM noise an rms value of

$$N_A \sim 18.2 \mu\text{s}.$$

Note that because of the assumptions made above, this is the same value as found for the inter-center difference between the two series at 50 mb.

All numerical weather prediction centers have access to the same suite of meteorological data. If these observations contain errors due to missing or inaccurate data (e.g. in the tropics or the Southern Hemisphere), a systematic AAM error may arise which cannot be detected by inter-center comparisons. The total AAM error is then taken to be

$$N_A = N_S + N_i$$

where N_S denotes the systematic component, common to all centers, and N_i is the inter-center error estimated above. Under the assumption that the systematic and inter-center errors are uncorrelated, the expected error variance becomes

$$\langle(L-X)^2\rangle = \langle N_i^2\rangle + \langle N_S^2\rangle,$$

where the interannual LOD error N_L has been neglected.

In a study of sub-seasonal variations in the Earth's angular momentum budget, *Dickey et al.* [1992b] found that systematic AAM error behaved as flicker noise, with a power spectral density of the form

$$P(f) = E_A(f_0/f),$$

where f_0 is a standard frequency ($= 0.1$ cycles/day), and $E_A \sim 0.009 \text{ ms}^2 (\text{cycles/day})^{-1}$. If we assume that this behavior extends to interannual frequencies, the power of the systematic error may be estimated as

$$N_s^2 = E_A f_0 \int_{f_1}^{f_2} \frac{df}{f} = E_A f_0 \ln \left(\frac{f_2}{f_1} \right) = 0.001 \text{ ms}^2,$$

where the frequency interval is bounded by the averaging time (1 year) and the length of the record considered (3 years). The resulting estimate for the systematic noise is $N_s = 31.6 \mu\text{s}$. However, the interannual AAM fluctuations may be more heavily influenced by data-poor regions (such as the stratosphere as shown by this study) than the sub-seasonal variations, which would increase the systematic noise.

Combining this value with the uncorrelated inter-center error estimated above gives a likely lower bound of about $37 \mu\text{s}$ for the interannual rms residual arising from noise in the AAM data. Residuals of 55 and $64 \mu\text{s}$ were found using the 1-mb wind-plus-pressure series for the EC and NMC, respectively, during the case study (cf. Table 1), implying the possible existence of an additional (uncorrelated) source of excitation with rms variation on the order of 40 to $50 \mu\text{s}$ when the EC or NMC data are considered. Possible oceanic contributions to this discrepancy are discussed in the following section.

4. Role of the Oceans

The analysis of the preceding section has shown that the dominant portion of the interannual LOD variation observed during the 1982-83 ENSO event can be explained by variations in globally-integrated atmospheric angular momentum (AAM). Furthermore, the lack of a significant delay between the AAM and LOD series examined in this study implies a relatively rapid exchange of angular momentum between the solid Earth and atmosphere. A significant portion of this exchange may occur directly over land, through frictional torque at the surface or pressure gradients acting across orography [Swinbank, 1985; Wahr, 1988]. Wolf and Smith [1988], in particular, presented evidence that rapid AAM

variations observed at the peak of the 1982-83 ENSO were produced by mountain torques acting over the Rockies. Furthermore, in a study of the AAM budget from a 20-year climate simulation using the Canadian Climate Centre general circulation model, *Boer* [1990] found that the dominant portion of angular momentum exchange on sub-annual time scales (in the model) occurred over land.

On the longest time scale resolved in *Boer's* analysis (1 year), however, the AAM variance explained by surface stress over the ocean was twice that associated with the combined friction and mountain torque over the land, indicating that ocean torques may predominate on interannual time scales. The ENSO cycle, in particular, is associated with pronounced fluctuations in the strength of the surface winds over the tropical oceans [e.g. *Lukas et al.*, 1983; *Wyrki*, 1985; *Philander*, 1990], with the largest AAM anomalies occurring in the sub-tropics [*Rosen et al.*, 1984; *Dickey et al.*, 1992]. If the bulk of the interannual AAM changes are associated with ENSO, as inferred in this and previous studies [e.g. *Chao*, 1984, 1988; *Eubanks et al.*, 1986], therefore, it is likely that a large fraction of the angular momentum exchanged with the solid Earth on these timescales is transmitted through the oceans.

Ponte [1990] has shown that the vertically-integrated torque on the ocean can be expressed in terms of external (barotropic) and internal (baroclinic) modes, and concluded that the barotropic modes dominate the oceanic angular momentum balance. The arguments of *Ponte* [1990] against the importance of baroclinic modes in the zonal angular momentum balance are not really applicable, however, both because *Ponte* ignores the mathematical question of convergence of his wind stress torque expansion, and because *Ponte* ignores the frequency dependent dynamical response of the various ocean modes to this forcing. Even if barotropic modes do dominate the long period ocean torque budget, quickly transmitting most of the total interannual wind stress torque to the solid Earth, at the same time significant amounts of angular momentum can still be accumulated by the slower interannual baroclinic waves. Large baroclinic modes are definitely excited as part of the

ENSO cycle, and (as will be shown below) these modes can certainly be significant in the angular momentum budget. In addition, therefore, to its role as an intermediary in the transmission of atmospheric stresses to the solid Earth, interannual changes in ocean circulation and mass distribution can also give rise to a separate dynamical contribution to the global angular momentum budget.

For the ENSO event of 1982-83, in particular, an imbalance of $\sim 25\%$ between the torques at the top and bottom of the oceans would be all that would be required to account for the 40-50 μs residual between the interannual LOD and AAM variations, assuming that the bulk of the total atmospheric stress on the solid Earth is actually transmitted through the oceans. Large changes in oceanic circulation were associated with the 1982-83 ENSO [*Philander*, 1990, and references therein]; in a study of sea-level variations during this event, *Wyrtki* [1985] used a two-layer approximation to the thermal structure of the tropical ocean to infer the presence of a zonal, 40-Sv current, flowing between the west- and east-tropical Pacific. Much of this water appeared to escape polewards, implying that recirculation may have occurred in basin-scale gyres rather than locally. For a return flow at latitude 45° , for example, such a current system would generate anomalies of $\sim 20 \mu\text{s}$ in LOD (see appendix), up to half the magnitude of the unexplained residual.

Changes in the mass distribution of the oceans may also be of sufficient magnitude to significantly influence the global angular momentum budget. In particular, the decimeter level variations observed in sea level during an El Niño event, together with the much larger simultaneous changes in thermocline depth, can be modeled as baroclinic waves [see *Kessler*, 1990]. Although sea level changes from local thermal expansion would not excite rotational variations, baroclinic changes caused by large scale redistributions of warm upper-level ocean water can modify the total mass content of the water column, leading to rotational effects. Baroclinic ocean modes have phase speeds of a few m/s, taking hundreds of days to years to propagate across the Pacific; hence these waves may play an important

role in the interchange of angular momentum among the atmosphere, ocean, and solid Earth on interannual time scales.

A rough estimate of the magnitude of these contributions can be made using a simple two-layer ocean model [e.g. *Gill*, 1982; *Eubanks*, 1993]. The two-layer model can be used to relate the integrated sea-level change in an area to the total change in the oceanic mass loading over the area, assuming that conditions are uniform across the area. This model supports a mode—the baroclinic mode—in which the changes in sea level and thermocline depth always oppose each other. For the baroclinic mode in the two-layer model, the ratio of the actual bottom pressure perturbation to the sea-level-induced pressure change is a constant, ϵ , which is always less than zero (i.e., the bottom pressure change is always dominated by the changes in thermocline depth). *Eubanks* [1993] applied this model to the equatorial Pacific and estimated that ϵ there is ~ -0.06 . During the 1983-83 event, a pulse of warm water similar to a barocline Kelvin wave propagated across the Pacific [*Wyrtki*, 1984; *Lukas et al.*, 1984], increasing the tropical sea level by 20 cm or more. Thus, in the two-layer model, this sea-level increase would be associated with a bottom pressure decrease of ~ 1.2 millibar, sufficient to significantly change the LOD, provided the perturbed area is large enough.

In his study of the 1982-83 ENSO event, *Wyrtki* [1985] found that the integrated tropical Pacific sea level decreased by $\sim 5 \times 10^{12} \text{ m}^3$ between $\pm 15^\circ$ latitude from late 1982 to mid-1983. Applying the calculated value of $\epsilon = -0.06$ indicates that the resulting equatorial mass load increased by $\sim 3 \times 10^{14} \text{ kg}$ during this time, equivalent to an LOD increase of $6.2 \mu\text{s}$ if the excess water comes from a globally uniform layer polewards of $\pm 15^\circ$ latitude (see appendix). *Luther* [personal communication] estimated $\epsilon \sim -0.25$ at 124°W at the equator; application of this value to the entire tropical Pacific gives an LOD increase of $\sim 26 \mu\text{s}$, comparable to the estimated current contribution. Since the LOD increased substantially from late 1982 to mid-1983 while the total AAM signal remained essentially

flat (see Fig. 4), such a contribution has the correct sign and timing to favorably impact the interannual LOD-AAM discrepancy.

Thus, the oceanic angular momentum contribution (including both moment-of-inertia changes transferred via baroclinic waves, and motion terms) must be considered a viable option to close the interannual axial angular momentum budget. The real ocean is considerably more complex than the simplified two-layer model considered here, having both continuous stratification and variations across the ocean basin [Philander, 1990], with a number of baroclinic modes to be considered [Cartwright *et al.*, 1987]. While a more quantitative evaluation of OAM changes during the 1982-83 ENSO event is beyond the scope of this study, it is clear that oceanic effects, though small, cannot be ignored in detailed determinations of the Earth's angular momentum budget on interannual time scales.

5. Summary

Interannual variations in the Earth's rate of rotation, and hence in the length-of-day (LOD), have previously been related to the El Niño/Southern Oscillation (ENSO) phenomenon through studies of the Southern Oscillation Index (SOI) [e.g. Chao, 1984, 1988; Eubanks *et al.*, 1986; Salstein and Rosen, 1986; Dickey *et al.*, 1993], and to the stratospheric Quasi-Biennial Oscillation (QBO) through an idealized model based on monthly wind data from three stations [Chao, 1989]. In this study we use time series of atmospheric angular momentum (AAM) up to 100 mb and 50 mb from the NMC and ECMWF operational analyses, combined with AAM estimates from 100 mb to 1 mb derived from satellite temperature soundings, to perform a case study of the Earth's interannual angular momentum budget during the unusually strong and well-observed 1982-83 ENSO.

A time-frequency analysis of LOD, AAM, and SOI data surrounding the 1982-83 event confirms the bimodal nature of the ENSO cycle found in previous studies [Rasmussen *et al.*, 1990; Barnett, 1991; Keppenne and Ghil, 1992; Dickey *et al.*, 1992a],

and indicates that the large amplitude of the 1982-83 event resulted from constructive interference between variations in a low-frequency (4-6 year) and a quasi-biennial (2-3 year) band. Atmospheric forcing was found to be the dominant cause of the associated rotational anomaly, with the AAM integrated up to 1 mb accounting for up to 92% of the interannual LOD variance from mid-1981 to mid-1984. The stratosphere was found to play an important role in the Earth's angular momentum budget on interannual time scales, accounting for ~ 20% of the LOD variance relative to the atmosphere below 100 mb; by contrast, variations in the atmospheric moment of inertia (the "pressure" term) played only a minor role, accounting for ~ 1% of the LOD variance. A small lag (10-20 days) in the LOD response to the full (1000 to 1 mb) AAM variation was found, but does not appear to be statistically significant.

The remaining 8-10% of the LOD variance (~ 55-64 μ s) cannot be accounted for with the existing atmospheric data sets, implying that exchange with another reservoir of angular momentum may play a significant role on these time scales, or that systematic problems exist with the current models and/or data sets. The difference between the interannual AAM variations from the NMC and ECMWF analyses integrated up to 50 mb (18.2 μ s rms) is a sizable fraction of the remaining LOD-AAM residual, implying that noise in the AAM data accounts for a significant portion of the residual. Systematic errors were estimated to be ~ 33 μ s by extrapolating the "flicker law" behavior of the subseasonal AAM error found by *Dickey et al.*, 1992b, to interannual time scales. Combining these error sources and assuming that errors in LOD values are negligible on interannual time scales gives a total expected LOD-AAM residual of 38 μ s, implying the possible existence of an additional uncorrelated source of excitation with an rms variation of 40 to 52 μ s, using the ECMWF and NMC data respectively. Oceanic angular momentum contributions (both moment-of-inertia changes transferred via baroclinic waves and motion terms) were shown to be promising candidates in closing the interannual axial angular momentum budget.

ACKNOWLEDGMENTS

We acknowledged interesting discussions with Y. Chao, I. Fukumori, and R. S. Gross. The authors thank D. A. Salstein for supplying the stratospheric AAM data used in our analysis. This paper presents the results of one phase of research carried out at the Jet Propulsion Laboratory, California Institute of Technology, sponsored by the National Aeronautics and Space Administration.

Appendix. Oceanic Angular Momentum Estimates

1. Effect of Currents

The axial angular momentum associated with a uniform oceanic current is

$$A_c = M[\mathbf{R} \times \mathbf{V}]_3$$

where M is the total mass contained in the current, and \mathbf{R} and \mathbf{V} are the position and velocity, respectively, with respect to an Earth-fixed frame of reference. For a zonal current at latitude θ the volumetric transport of the current is

$$F = M|\mathbf{V}| / \rho a \cos \theta \Delta\lambda ,$$

where a is the Earth's radius, ρ is the density and $\Delta\lambda$ is the longitudinal extent of the current, allowing the angular momentum to be written as

$$A_c = \rho F a^2 \cos^2\theta \Delta\lambda ;$$

for an idealized gyre consisting of a flow along the equator joined to a counter-flow at latitude θ by meridional currents. In particular, the net angular momentum is

$$A_c = \rho F a^2 (1 - \cos^2\theta) \Delta\lambda .$$

Expressing the oceanic transport in Sverdrups ($1 \text{ Sv} = 10^6 \text{ m}^3/\text{sec} \sim 10^9 \text{ kg}/\text{sec}$), the corresponding change in the length-of-day is given by

$$\Delta\Lambda = 1.67 \times 10^{-29} A_c \sim 1.67 \times 10^{-20} F a^2 \sin^2\theta \Delta\lambda ;$$

for a gyre with longitudinal extent of 90° and return flow at latitude 45° this gives

$$\Delta\Lambda \sim F/2 \times 10^{-6} \text{ sec},$$

or about $20 \mu\text{s}$ for a total transport of 40 Sv .

2. Effect of Mass Displacements

The planetary angular momentum per unit mass at latitude θ is

$$A(\theta) = \Omega a^2 \cos^2 \theta ,$$

where Ω and a are the angular velocity and radius of the Earth, respectively. For a uniform distribution of mass between latitudes θ_1 and θ_2 , the average angular momentum per unit mass is

$$\bar{A} = \Omega a^2 \frac{\int_{\theta_1}^{\theta_2} \cos^3 \theta d\theta}{\int_{\theta_1}^{\theta_2} \cos \theta d\theta} ;$$

the displacement of a unit mass from the polar cap ($\Theta, 90^\circ$) to the tropical belt ($-\Theta, \Theta$) can be shown to give an average change in angular momentum per unit mass of

$$\delta \bar{A} = \frac{\Omega a^2}{3} (1 + \sin \Theta) .$$

For $\Theta = 15^\circ$, the resulting change in the length-of-day is

$$\Delta \Lambda = 1.67 \times 10^{-29} \delta A = 2.06 \times 10^{-20} \text{ sec/kg},$$

yielding an estimated LOD change of

$$\Delta \Lambda \sim 6 \mu\text{s}$$

for the mass increase of 3×10^{14} kg calculated from Wyrтки's sea-level data using the factor $\epsilon = -0.06$, and

$$\Delta \Lambda \sim 26 \mu\text{s}$$

for the mass increase calculated using the value $\epsilon = -0.25$.

REFERENCES

- Barnes, R. T. H., R. Hide, A. A. White, and C. A. Wilson, Atmospheric Angular Momentum Fluctuations, Length of Day Changes and Polar Motion, *Proc. R. Soc. London*, **A387**, 31-73, 1983.
- Barnett, T. P., The Interaction of Multiple Time Scales in the Tropical Climate System, *J. Climate*, **4**, 269-288, 1991.
- Bloomfield, P., *Fourier Analysis of Time Series: An Introduction*, John Wiley & Sons, New York, 1976.
- Cartwright, D. E., R. Spencer, and J. M. Vassie, Pressure Variations on the Atlantic Equator, *J. Geophys. Res.*, **92**, 725-741, 1987.
- Cazenave, A. (ed.), *Earth Rotation: Solved and Unsolved Problems, NATO Advanced Institute Series C: Mathematical and Physical Sciences Vol. 187*, ed. A. Cazenave, D. Reidel, Boston, 1986.
- Chao, B. F., Interannual Length-of-Day Variations with Relation to the Southern Oscillation/El Niño, *Geophys. Res. Lett.*, **11**, 541-544, 1984.
- Chao, B. F., Correlation of Interannual Lengths-of-Day Variation with El Niño/Southern Oscillation, 1972-1986, *J. Geophys. Res.*, **93**, B7, 7709-7715, 1988.
- Chao, B. F., Length-of-Day Variations Caused by El Niño/Southern Oscillation and the Quasi-Biennial Oscillation, *Science*, **243**, 923-925, 1989.
- Chen, W. Y., Assessment of Southern Oscillation Sea-Level Pressure Indices., *Mon. Weather Rev.*, **110**, 800-807, 1982.
- Dickey, J. O., and T. M. Eubanks, The Application of Space Geodesy to Earth Orientation Studies, *Space Geodesy and Geodynamics* (eds.) by A. J. Anderson and A. Cazenave, Academic Press, New York, 221-269, 1986.
- Dickey, J. O., T. M. Eubanks, and R. Hide, Interannual and Decade Fluctuations in the Earth's Rotation, *Variations in the Earth's Rotation, Geophysical Monograph Series of the American Geophysical Union*, Washington, D. C. McCarthy (ed.), 157-162, 1990.
- Dickey, J. O., S. L. Marcus and R. Hide, Global Propagation of Interannual Fluctuations in Atmospheric Angular Momentum, *Nature*, **357**, 482-488, 1992a.
- Dickey, J. O., S. L. Marcus, J. A. Steppe, and R. Hide, The Earth's Angular Momentum Budget on Subseasonal Time Scales, *Science*, **255**, 321-324, 1992b.
- Dickey, J. O., Atmospheric Excitation of the Earth's Rotation: Progress and Prospects via Space Geodesy, *Space Geodesy and Geodynamics, Geophysical Monograph of the American Geophysical Union*, ed., D. Turcotte, Washington D. C., in press, 1993.
- Dickey, J. O., S. L. Marcus, T. M. Eubanks, and R. Hide, Climate Studies Via Space Geodesy: Relationships Between ENSO and Interannual Length-of-Day Variations, *Am. Geophys. Un. Mono. 75, IUGG Symposium Volume 15, Interactions Between Global Climate Subsystems: The Legacy of Hann*, Eds. G. A. Bean and M. Hantell, Washington, D. C., 141-155, 1993.

- Eubanks, T. M., J. O. Dickey, and J. A. Steppe, The 1982-83 El Niño, the Southern Oscillation, and Changes in the Length of Day, *Trop. Ocean and Atmos. Newsletter*, **29**, 21-23, 1985a.
- Eubanks, T. M., J. O. Dickey, J. A. Steppe, and P. S. Callahan, A Spectral Analysis of the Earth's Angular Momentum Budget, *J. Geophys. Res.*, **90**, B7, 5385-5404, 1985b.
- Eubanks, T. M., J. A. Steppe, and J. O. Dickey, The El Niño, the Southern Oscillation and the Earth's Rotation, in *Earth Rotation; Solved and Unsolved Problems, NATO Advanced Institute Series C: Mathematical and Physical Sciences*, **187**, ed. A. Cazenave, 163-186, D. Reidel, Hingham, Mass., 1986.
- Eubanks, T. M., Variations in the Orientation of the Earth, *Space Geodesy and Geodynamics Geophysical Monograph of the American Geophysical Union*, ed., D. Turcotte, Washington D. C., in press, 1993.
- Gross, R. S., A Combination of Earth Orientation Data: SPACE91, in *IERS Technical Note 11: Earth Orientation Reference Frame, Atmospheric Excitation Functions, (submitted for the 1991 IERS Annual Report)* (Annex to the IERS Annual Report for 1991), ed. P. Charlot, in press, Observatoire de Paris, Paris, France, 1992.
- Hide, R., Towards a Theory of Irregular Variations in the Length of the Day and Core-Mantle Coupling, *Phil. Trans. Roy. Soc.*, **A284**, 547-554, 1977.
- Hide, R., Rotation of the Atmospheres of the Earth and Planets, *Phil. Trans. R. Soc. Lond.* **A313**, 107-121, 1984.
- Hide, R., Presidential Address: The Earth's Differential Rotation, *Quart. J. Roy. Astron. Soc.*, **278**, 3-14, 1986.
- Hide, R., and J. O. Dickey, Earth's Variable Rotation, *Science*, **253**, 629, 1991.
- Hirota, I., T. Hirooka, and M. Shiotani, Upper Stratospheric Circulations in the Two Hemispheres Observed by Satellites, *Q. J. R. Meteorol. Soc.*, **109**, 443-454, 1983.
- Horel, J. D., and J. M. Wallace, Planetary-Scale Atmospheric Phenomena Associated with the Southern Oscillation, *Mon. Weather Rev.*, **109**, 813-828, 1981.
- Keppenne, C. L., and M. Ghil, Adaptive Filtering and Prediction of the Southern Oscillation Index, *J. Geophys. Res.*, **97**, 20,449-20,454, 1992.
- Kessler, W. S., Observations of Long Rossby Waves in the Northern Tropical Pacific, *J. Geophys. Res.*, **95**, 5183-5217, 1990.
- Lambeck, K., *The Earth's Variable Rotation*, Cambridge Univ. Press, London and New York, 1980.
- Lambeck, K., *Geophysical Geodesy, The Slow Deformation of the Earth*, Clarendon Press, Oxford, 1988.
- Lambeck, K., and A. Cazenave, The Earth's Rotation and Atmospheric Circulation, I, Seasonal Variations, *J. R. Astron. Soc.*, **32**, 79-93, 1973.

- Lukas, R., S. P. Hayes, and K. Wyrski, Equatorial Sea Level Response During the 1982-1983 El Niño, *J. Geophys. Res.*, **89**, 10425-10430, 1984.
- Meehl, G. A., Air-Sea Biennial Mechanism in the Tropical Indian and Pacific Region—Role of the Ocean, *J. Climate*, **6**, 1, 31-41, 1993.
- Morabito, D. D., T. M. Eubanks, and J. A. Steppe, Kalman Filtering of Earth Orientation Changes. *The Earth's Rotation and Reference Frames for Geodesy and Geodynamics*, A. K. Babcock and G. A. Wilkins, Kluwer Academic Publishers, Dordrecht, 257-268, 1988.
- Moritz, H., and I. I. Mueller, *Earth Rotation: Theory and Observation*, The Ungar Publishing Co., New York, 1987.
- Munk, W. H., and G. J. F. MacDonald, *The Rotation of the Earth*, Cambridge University Press, 1960.
- Murakami, M., Large-scale Aspects of Deep Convective Activity Over the GATE Area, *Mon. Wea. Rev.*, **107**, 994-1013, 1979.
- Philander, S. G. H., El Niño Southern Oscillation Phenomena, *Nature*, **302**, 295-301, 1983.
- Philander, S. G. H., *El Niño, La Niña, and the Southern Oscillation*, Academic Press, New York, 1990.
- Rasmusson, E. U., and J. M. Wallace, Meteorological Aspects of the El Niño/Southern Oscillation, *Science*, **222**, 1195-1202, 1983.
- Rasmusson, E. M., X. Wang, and C. F. Ropelewski, The Biennial Component of ENSO Variability, *J. Mar. Systems*, **1**, 71-96, 1990.
- Rochester, M. G., Causes of Fluctuations in the Earth's Rotation, *Phil. Trans. R. Soc. Lond.*, **A313**, 95-105, 1984.
- Rosen, R. D., D. A. Salstein, T. M. Eubanks, J. O. Dickey, and J. A. Steppe, An El Niño Signal in Atmospheric Angular Momentum and Earth Rotation, *Science*, **225**, 411-414, 1984.
- Rosen, R. D., and D. A. Salstein, Contribution of Stratospheric Winds to Annual and Semi-Annual Fluctuations in Atmospheric Angular Momentum and the Length of Day, *J. Geophys. Res.*, **90**, 8033-8041, 1985.
- Rosen, R. D., D. A. Salstein, A. J. Miller, and K. Arpe, Accuracy of Atmospheric Angular Momentum Estimates from Operational Analyses, *Mon. Wea. Rev.*, **115**, 1627-1639, 1987.
- Rosen, R. D., D. A. Salstein, T. M. Wood, Discrepancies in the Earth-Atmosphere Angular Momentum Budget, *J. Geophys. Res.*, **95**, 265-279, 1990.
- Rosen, R. D., The Axial Momentum Balance of Earth and its Fluid Envelope, *Surveys Geophys.*, **14**, 1-29, 1993.

- Salstein, D. A., and R. D. Rosen, Earth Rotation as a Proxy for Interannual Variability in Atmospheric Circulation, 1860-Present, *J. Clim. and Appl. Meteorol.*, **25**, 1870-1877, 1986.
- Salstein, D. A., D. M. Kann, A. J. Miller, and R. D. Rosen, The Sub-Bureau for Atmospheric Angular Momentum of the International Earth Rotation Service: A meteorological data center with geodetic applications, *Bull. Amer. Meteor. Soc.*, **74**, 67-80, 1993.
- Stephnic, M., Interannual Atmospheric Angular Momentum Variability 1963-1973 and the Southern Oscillation, *J. Geophys. Res.*, **87**, 428-432, 1982
- Swinbank, R., The Global Atmospheric Angular Balance Inferred from Analysis Made During GFFE, *Quart. J. R. Met. Soc.*, **111**, 977-992, 1985.
- Wahr, J. M., The Earth's Rotation, *Ann. Rev. Earth Planet Sci.*, **16**, 231-249, 1988.
- Wyrski, K., The Slope of Sea Level Along the Equator During the 1982/1983 El Niño, *J. Geophys. Res.*, **89**, 10419-10424, 1984.
- Wyrski, K., Water Displacements in the Pacific and the Genesis of El Niño Cycles, *J. Geophys. Res.*, **90**, 7129-7132, 1985.
- Xu, J. S., On the Relationship Between the Stratospheric Quasi-Biennial Oscillation and the Tropospheric Southern Oscillation, *J. Atmos. Sci.*, **49**, 9, 725-734, 1992.

Table 1
Study of the 1982-83 ENSO Event
LOD variance explained by Atmospheric Angular Momentum

	Center	Components Used	Residual (ms) LOD-AAM	Variance Explained
Total (1000 to 1mb)	EC*	W	0.0590	90.7%
		W+P	0.0549	91.9%
	NMC*	W	0.0655	88.5%
		W+P	0.0641	89.0%
		W+P (IB)	0.0680	87.6%
	Contribution to 50 mb (1000-50mb)	EC	W	0.0772
W+P			0.0758	84.6%
NMC		W	0.0903	78.1%
		W+P	0.0896	78.4%
		W+P (IB)	0.0955	75.5%
Contribution to 100 mb (1000-100mb)		EC	W	0.1008
	W+P		0.0991	73.0%
	NMC	W	0.1055	70.1%
		W+P	0.1047	70.6%
		W+P (IB)	0.1105	67.2%

Yearly moving average detrended for both the LOD and AAM series

Total LOD variance = 0.1930 msec

Time series considered: 1981.5-1984.5

EC ≡ European Center for Medium-Range Weather Forecasts

NMC ≡ National Meteorological Center (US)

W = Wind terms

P = Pressure terms

IB ≡ Inverted barometer assumption assumed

* EC and NMC have common data from 100 to 1 mb (see text)

LEGENDS FOR FIGURES

Fig. 1. Time series of irregular fluctuations in the length-of-day $\Lambda^*(t)$ (curve (A)) and its decadal ($\Lambda_\alpha(t)$), interannual ($\Lambda_\beta(t)$), seasonal ($\Lambda_\gamma(t)$), and intraseasonal ($\Lambda_\delta(t)$) components (curves (B), (C), (D) and (E) respectively) updated from *Hide and Dickey* [1991].

Fig. 2. The interannual LOD variation, Λ^*_β (computed as the one-year moving average minus the five-year moving average — upper curve), compared to the negative of the interannual variation in the Southern Oscillation Index (MSOI — lower curve).

Fig. 3. Length-of-day from the JPL Kalman smoothing of space geodetic measurements as well as that inferred from atmospheric angular momentum from the National Meteorological Center (NMC) analysis for the period 1976 through 1991, together with a 365-day moving average which allows comparison on interannual time scales. Variation in the residual is shown by the lower curve.

Fig. 4. (a) Variations in a daily time series of LOD (solid line), smoothed with a tapered 365-day running average to remove seasonal variability, and detrended to remove decadal variability. Also shown are similarly smoothed variations in daily AAM from the EC operational analysis extending to 100 mb and to 50 mb (dashed lines — wind term only; dash-dot lines — wind plus pressure), and variations up to 1 mb formed by adding the stratospheric series to the 100-mb values. (b) as in (a), for the NMC operational analysis (dotted line — wind-plus-pressure calculated with the inverted barometer (IB) assumption).

Fig. 5. Fractional variance of the LOD series in Fig. 4 explained by the AAM series based on (a) NMC and (b) EC operational analyses to the 100-mb and 50-mb levels, and by variations up to 1 mb formed by adding the stratospheric series to the 100-mb values. A lower bound on

the uncertainty (dotted lines) is computed as the difference in the maximum variance explained by the 1-mb series incorporating NMC and EC data. Since the difference between the maximum explained variance and the explained variance at zero-lag for each center falls within this band, the LOD lag with respect to the 1-mb series considered here is not significant.

Fig. 6. (a) Interannual variations in a monthly time series of normalized LOD values for the period 1976-1991, filtered recursively [Murakami, 1979] in 8 equal-frequency bands ranging from 0.1 to 0.9 cycles per year. (b) as in (a), for the modified Southern Oscillation Index. (c) as in (a), for the tropospheric (1000–100 mb) AAM from the operational NMC analysis. (d) as in (a), for the stratosphere (100–1 mb).

Fig. 7. (a) Variations in a monthly time series of LOD, filtered recursively [Murakami, 1979] in the LF (32-88 month — dashed line) and QB (18-35 month — dotted line) bands defined by Barnett [1991]. The full interannual variation (sum of the LF and QB components) is shown by the solid line. (b) as in (a), for the modified Southern Oscillation Index. (c) as in (a), for the tropospheric (1000–100 mb) AAM from the operational NMC analysis. (d) as in (a), for the stratospheric (100–1 mb) AAM inferred from satellite temperature soundings. (e) The full interannual variation (sum of the LF and QB components) for tropospheric (1000–100 mb) AAM (dashed line), stratospheric (100-1 mb) AAM, and the total (1000–1 mb) AAM (solid line).

SPECTRAL COMPONENTS OF LOD

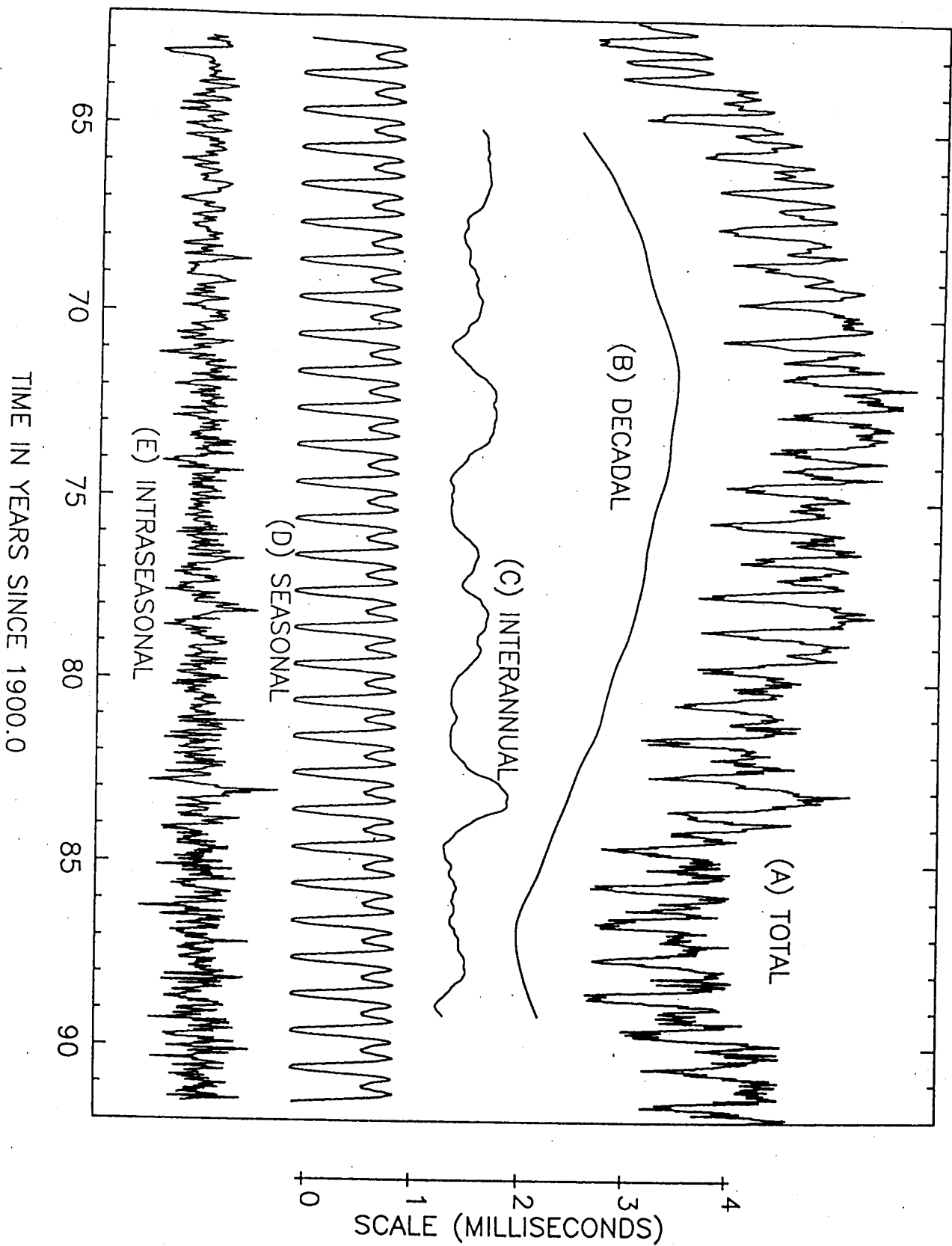


FIG 1

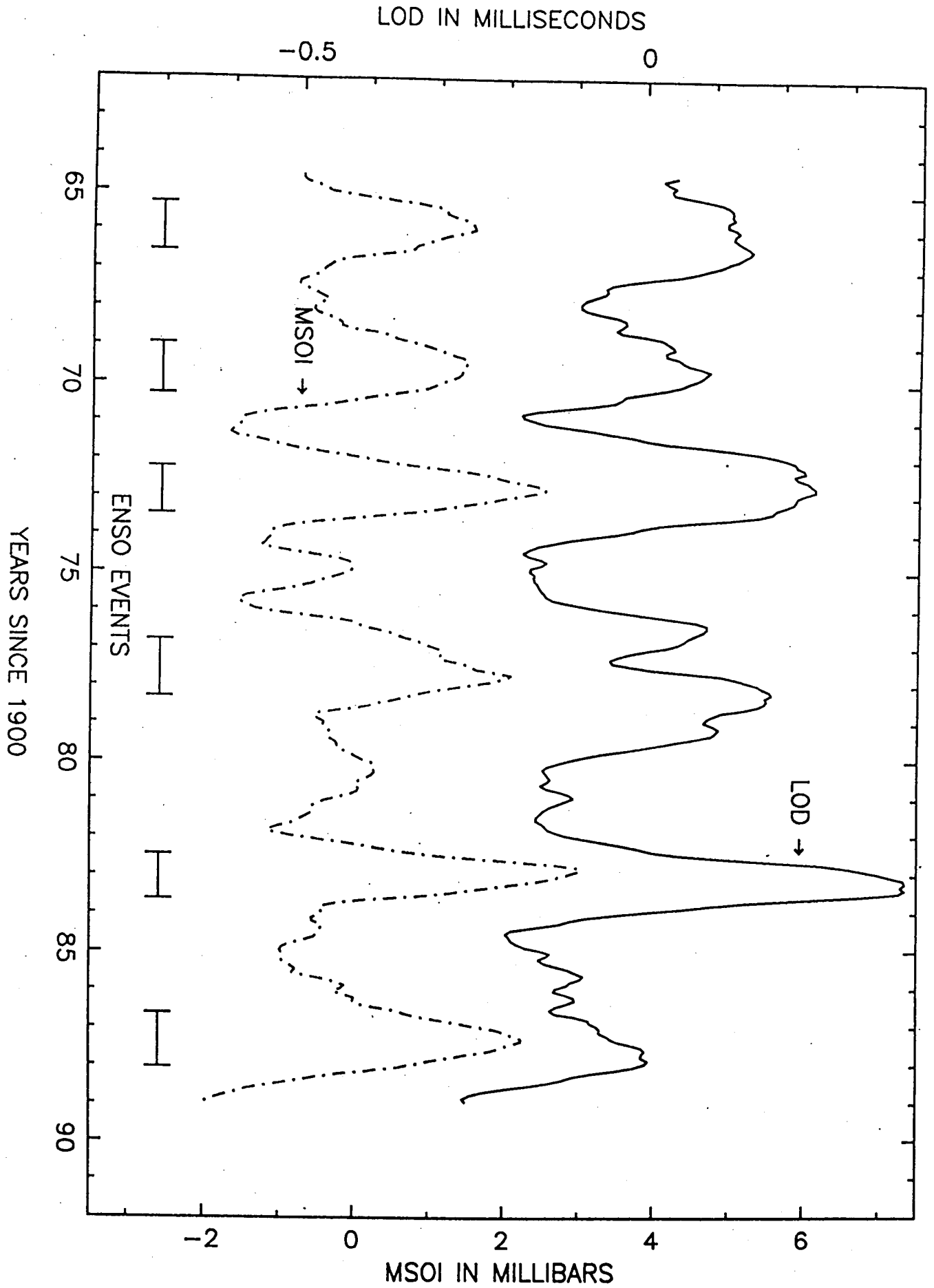


FIG 2

LOD/AAM VARIATION

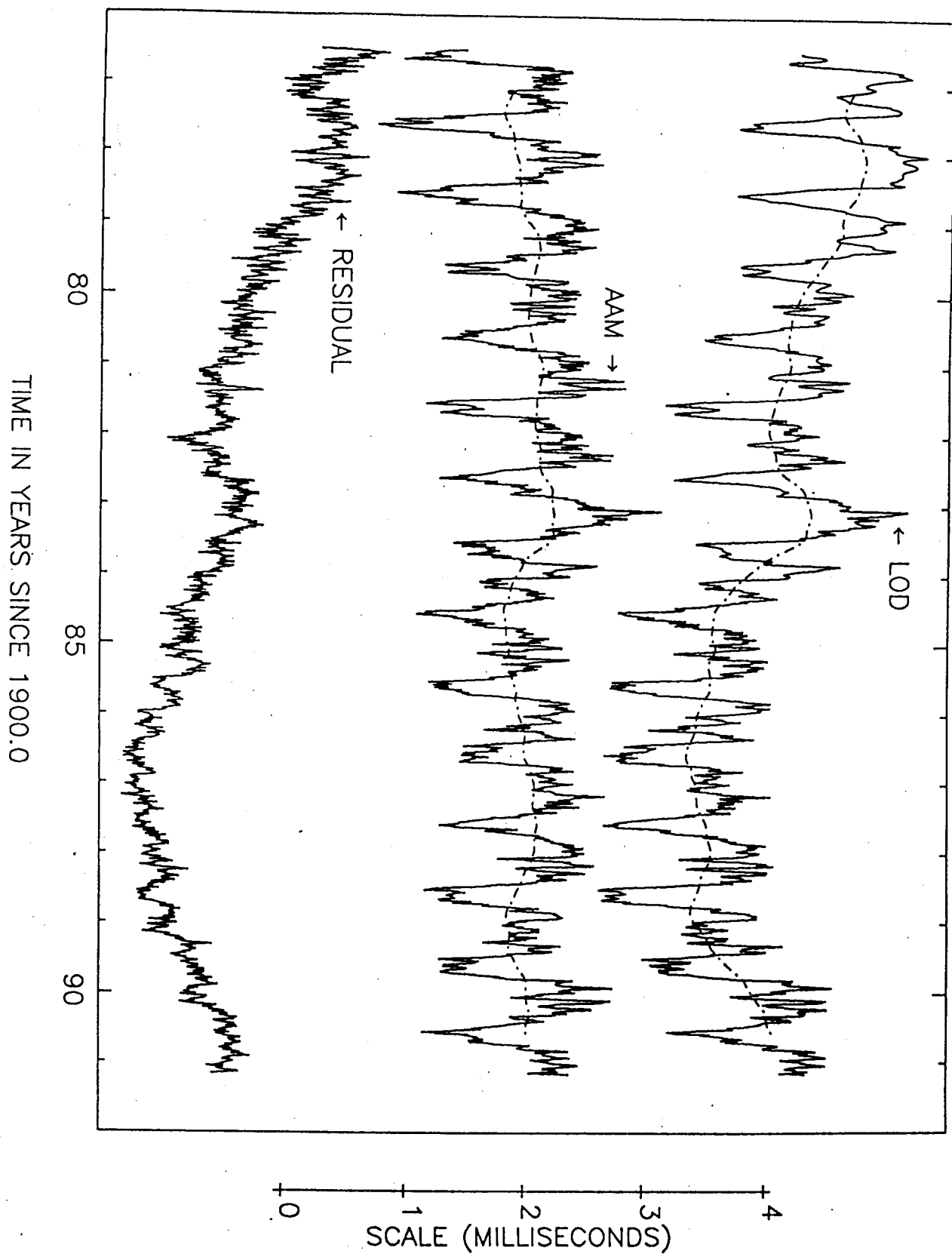


FIG 3

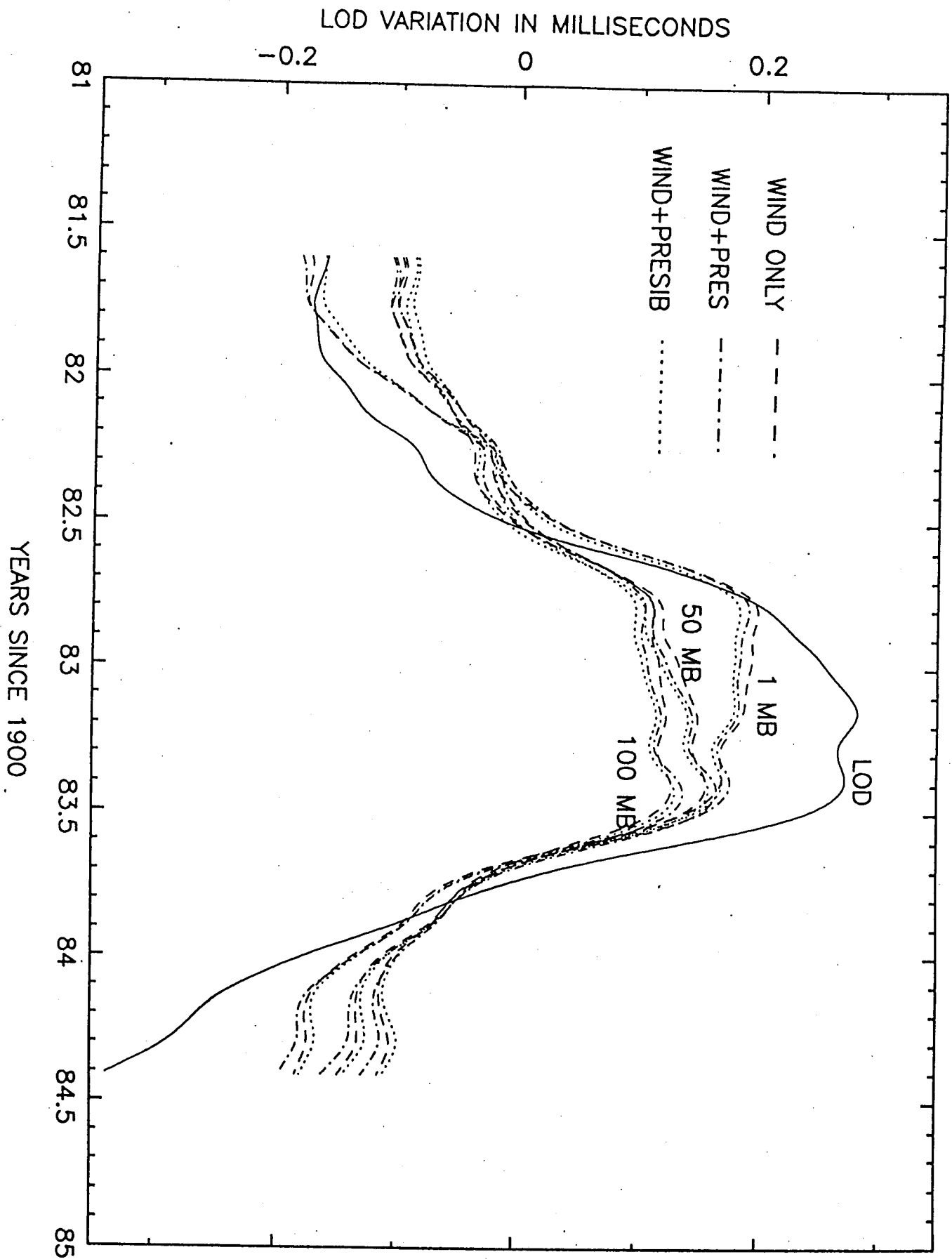


FIG 9 a

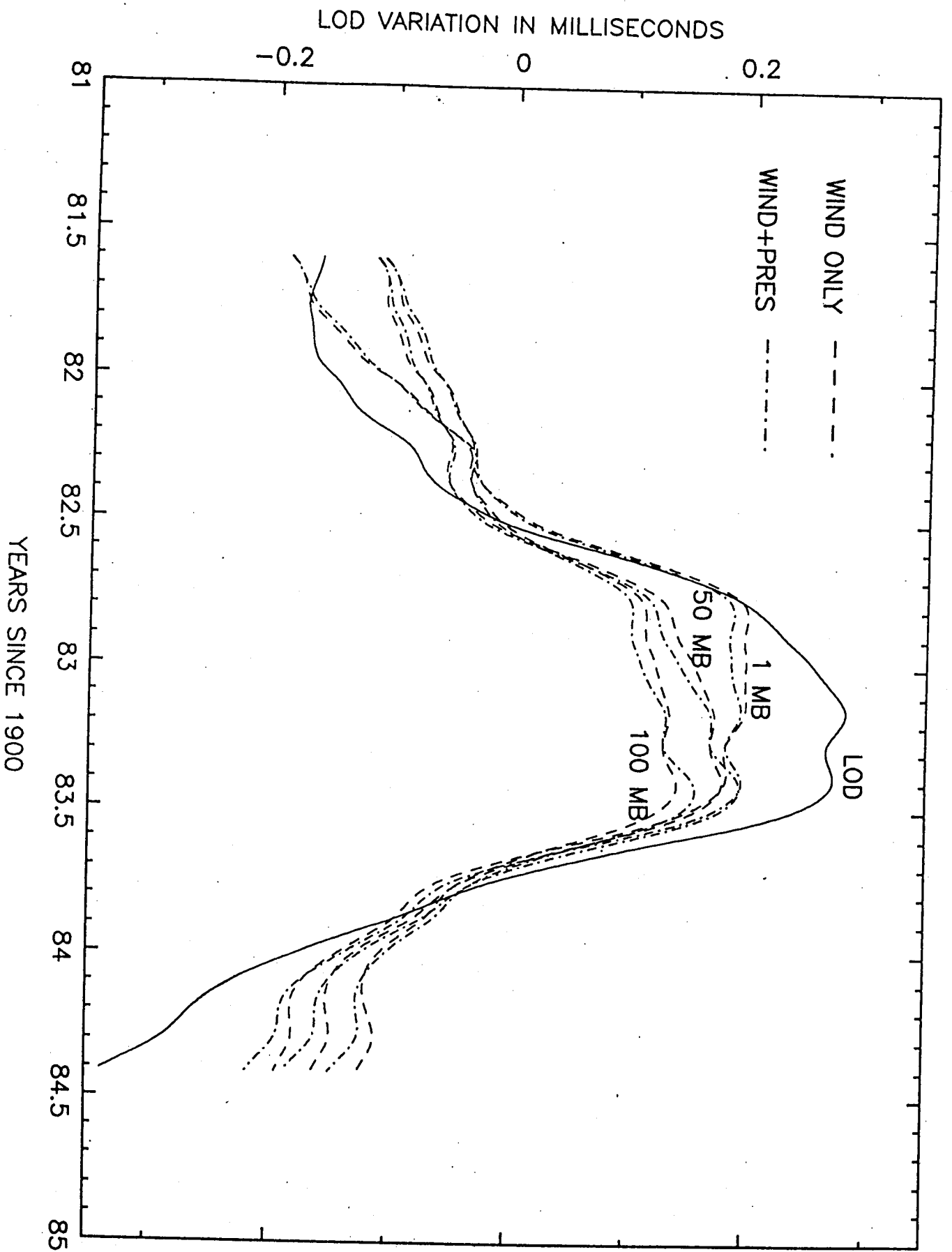


Fig 4b

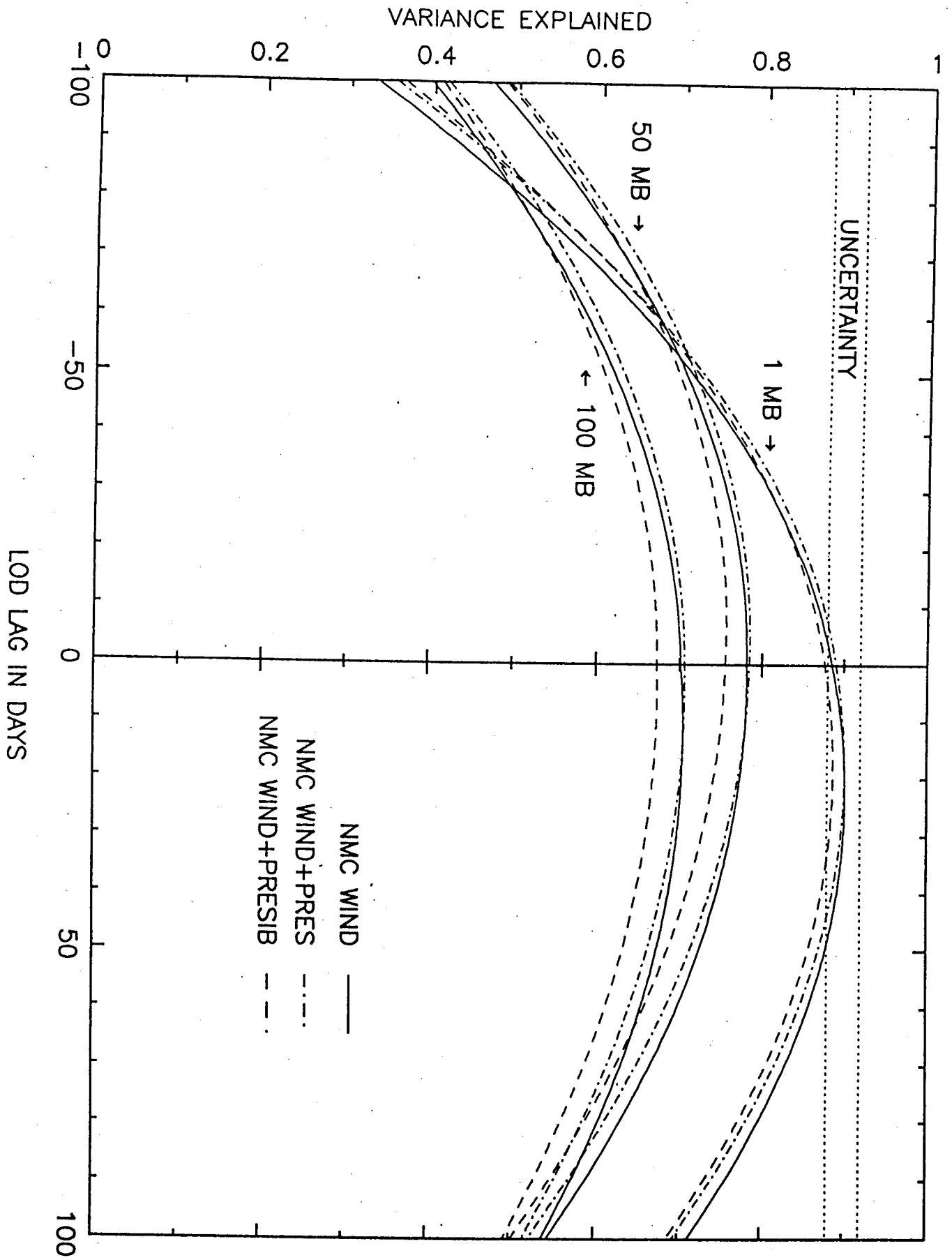


Fig 5a

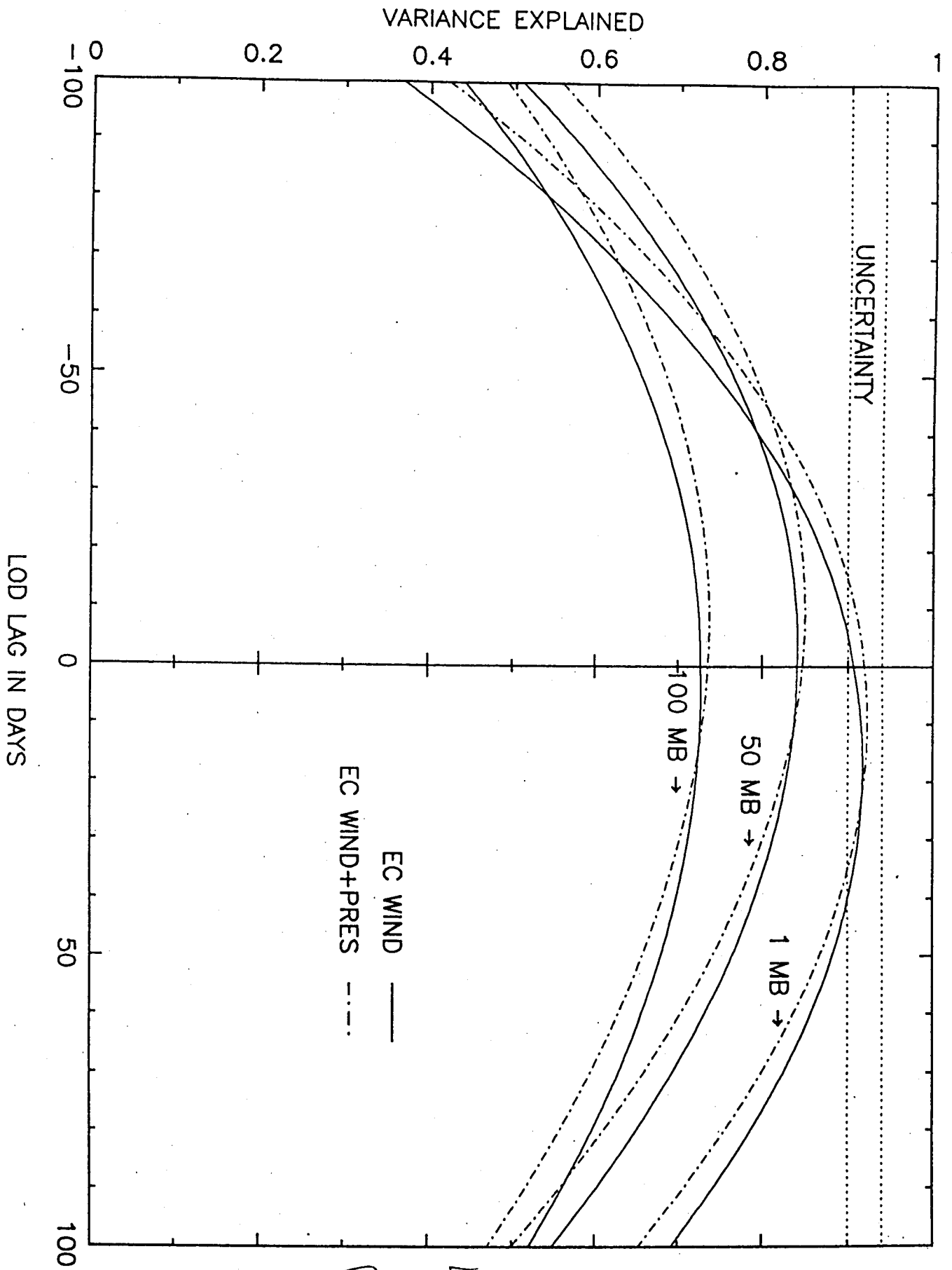
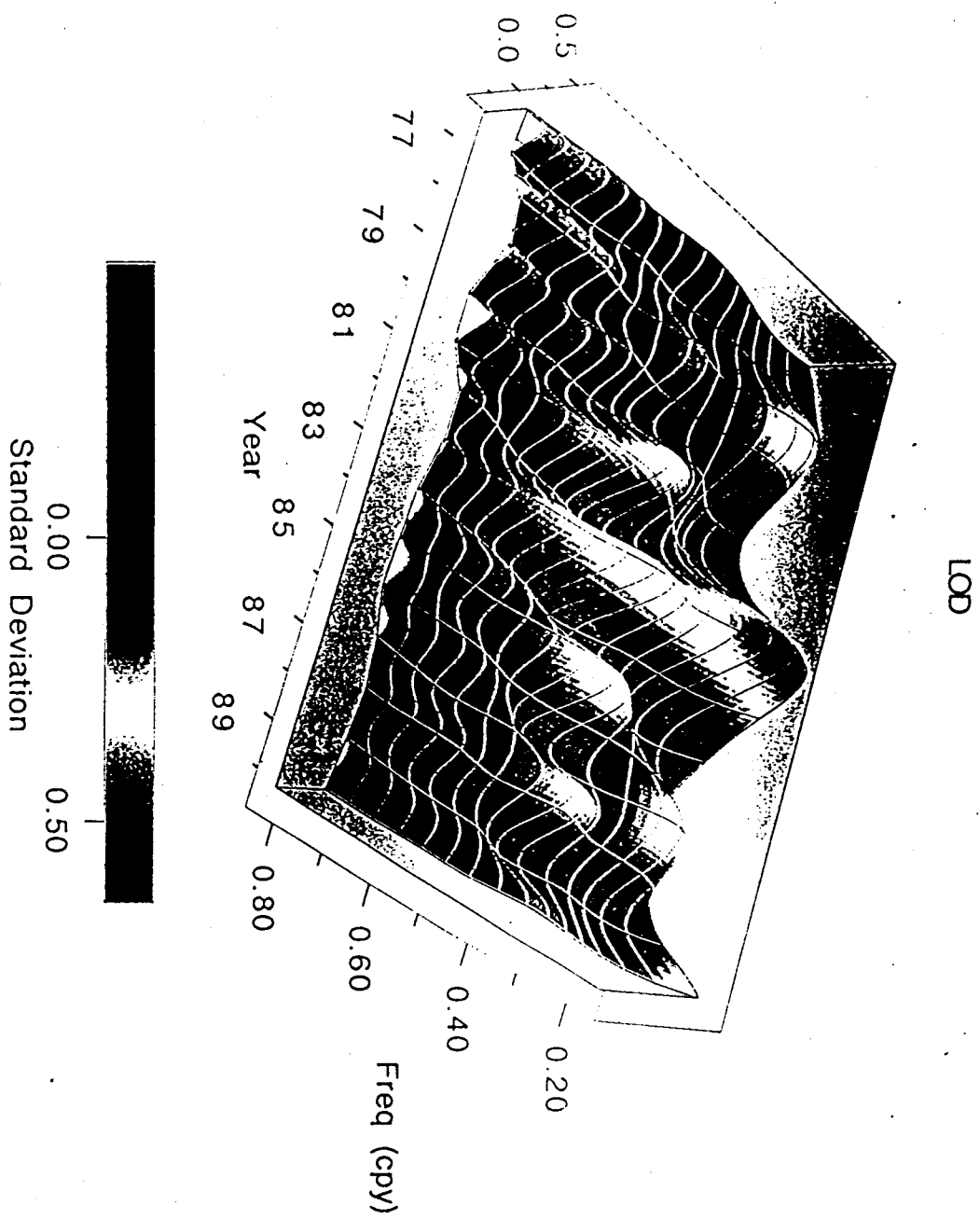


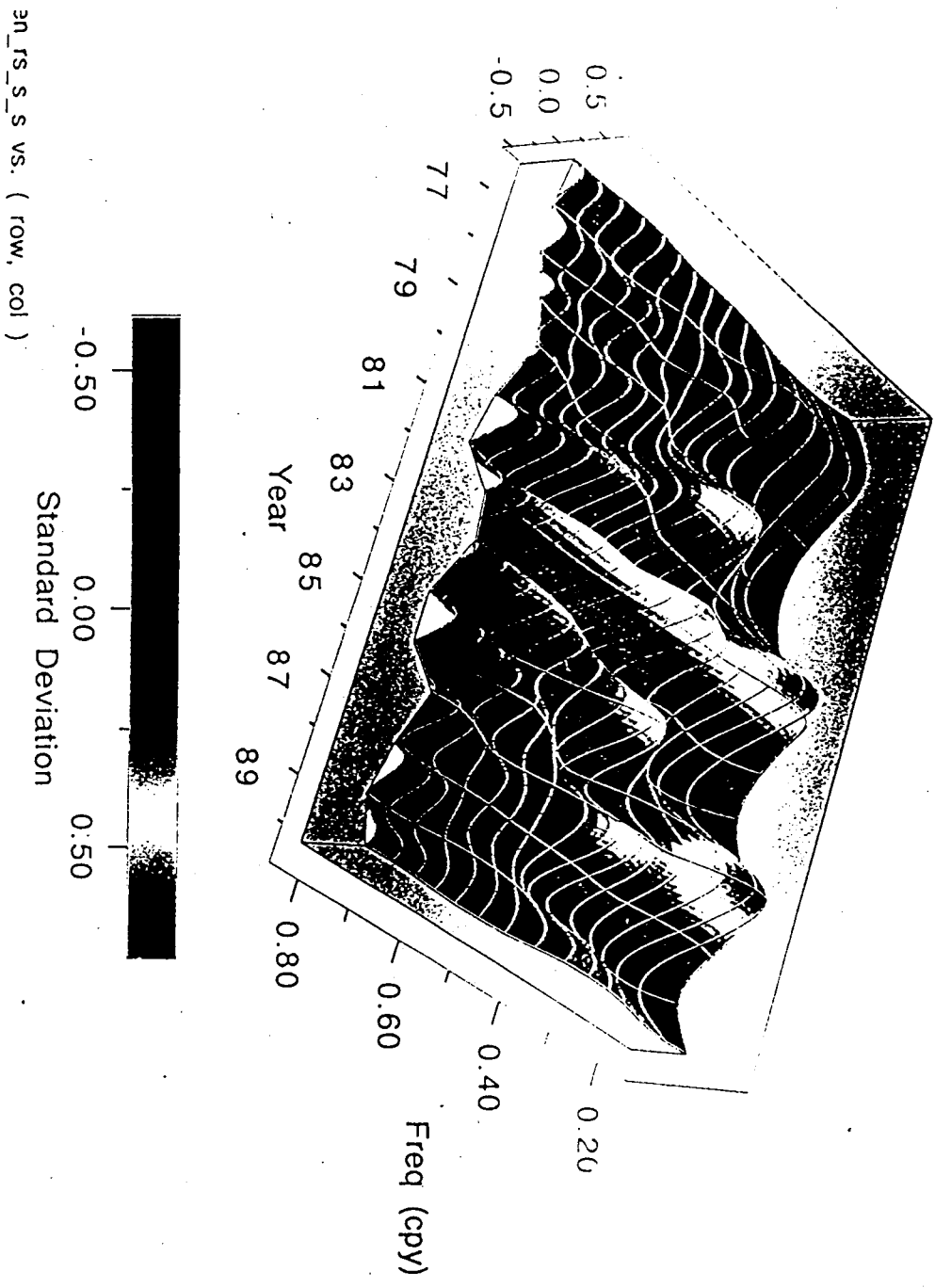
Fig 5b



ven_rs_s_s vs. (row, col)

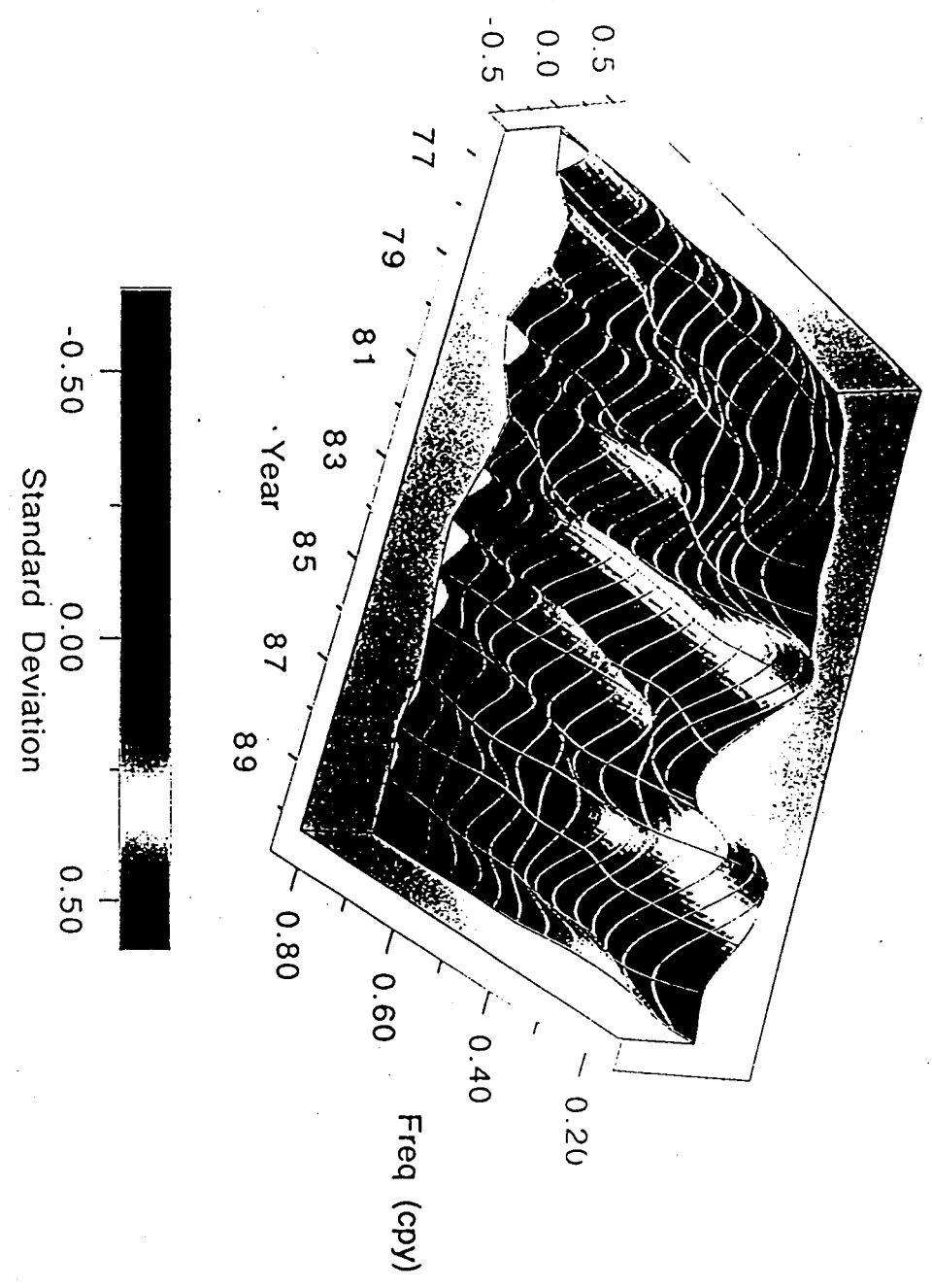
Fig 6a

Modified SOI



Fj 6b

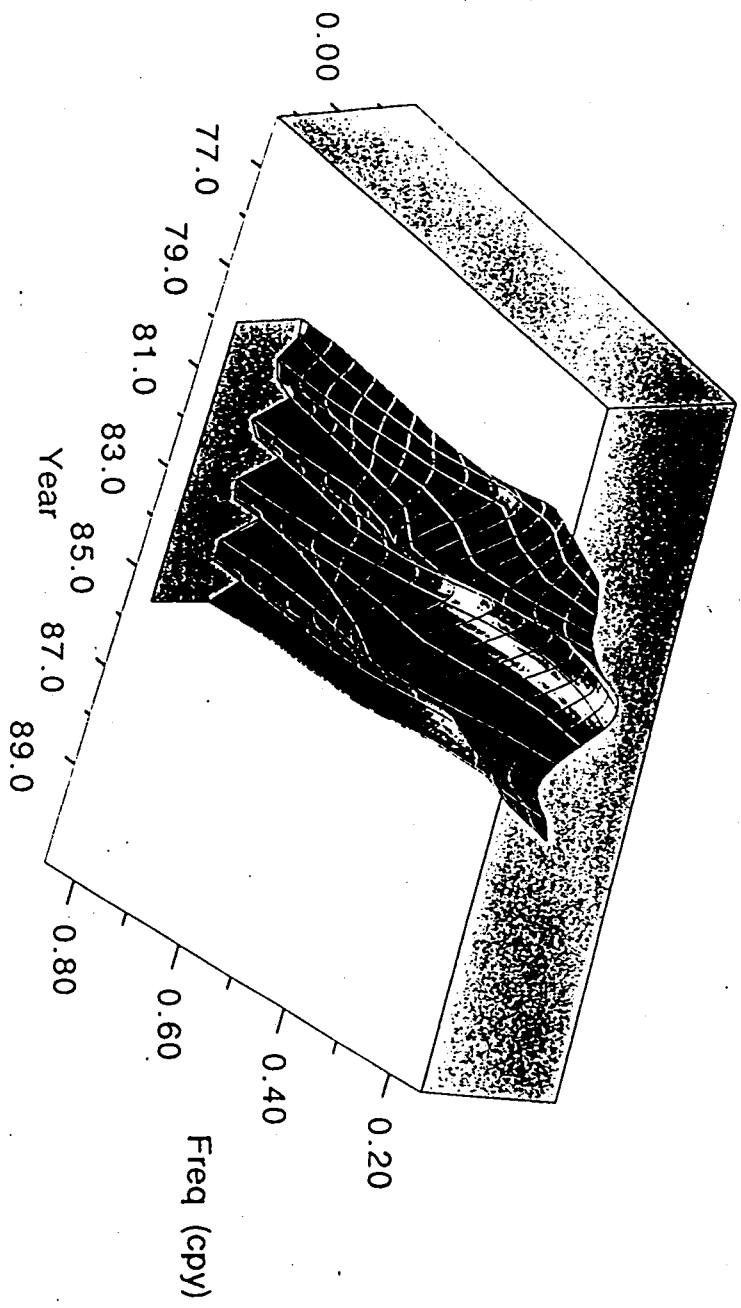
Tropospheric AAM



en_rs_s_s vs. (row, col)

Fig 6c

strat_waven_rs_s



strat_waven_rs_s vs. (row, col)

Fig 6d

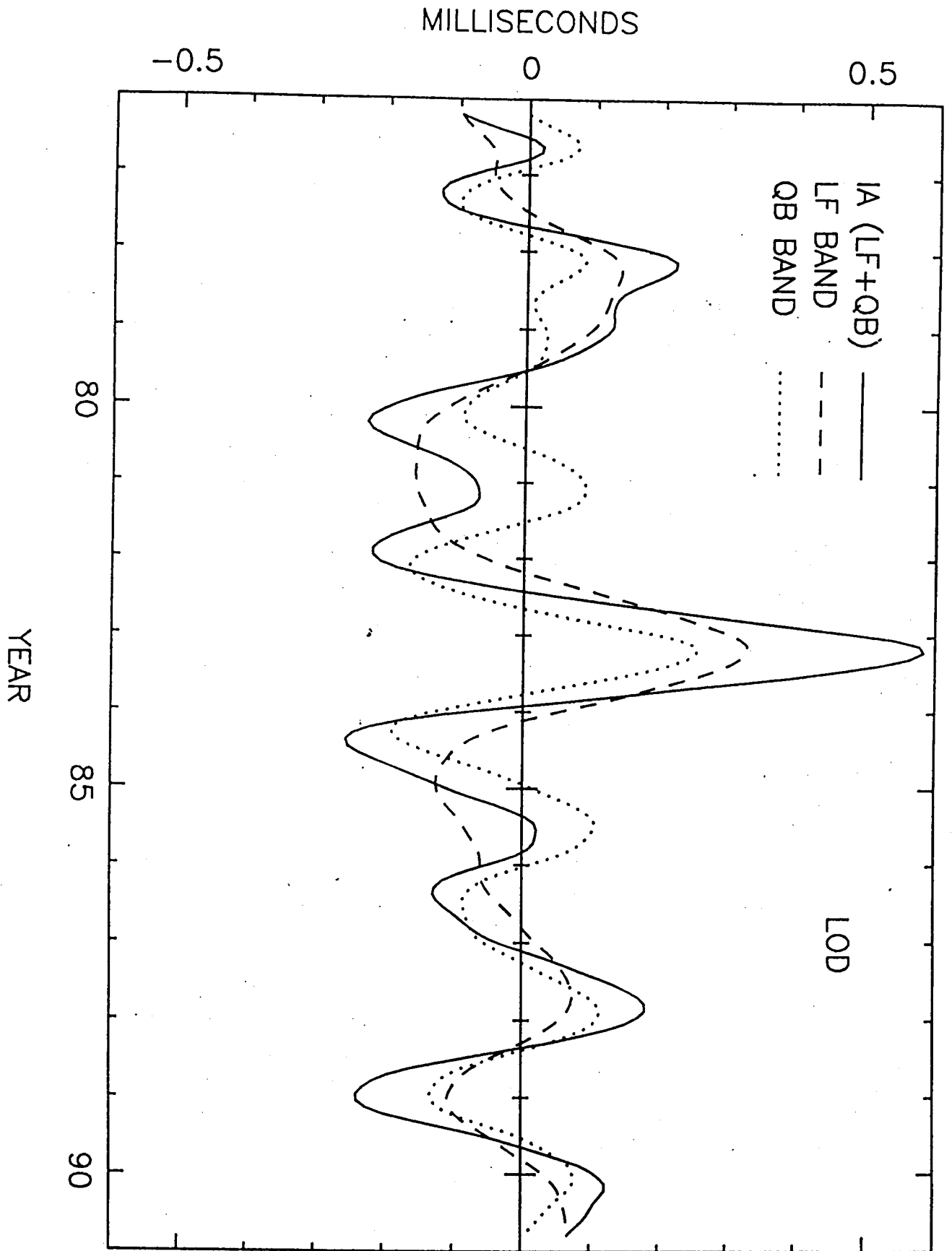


Fig 7a

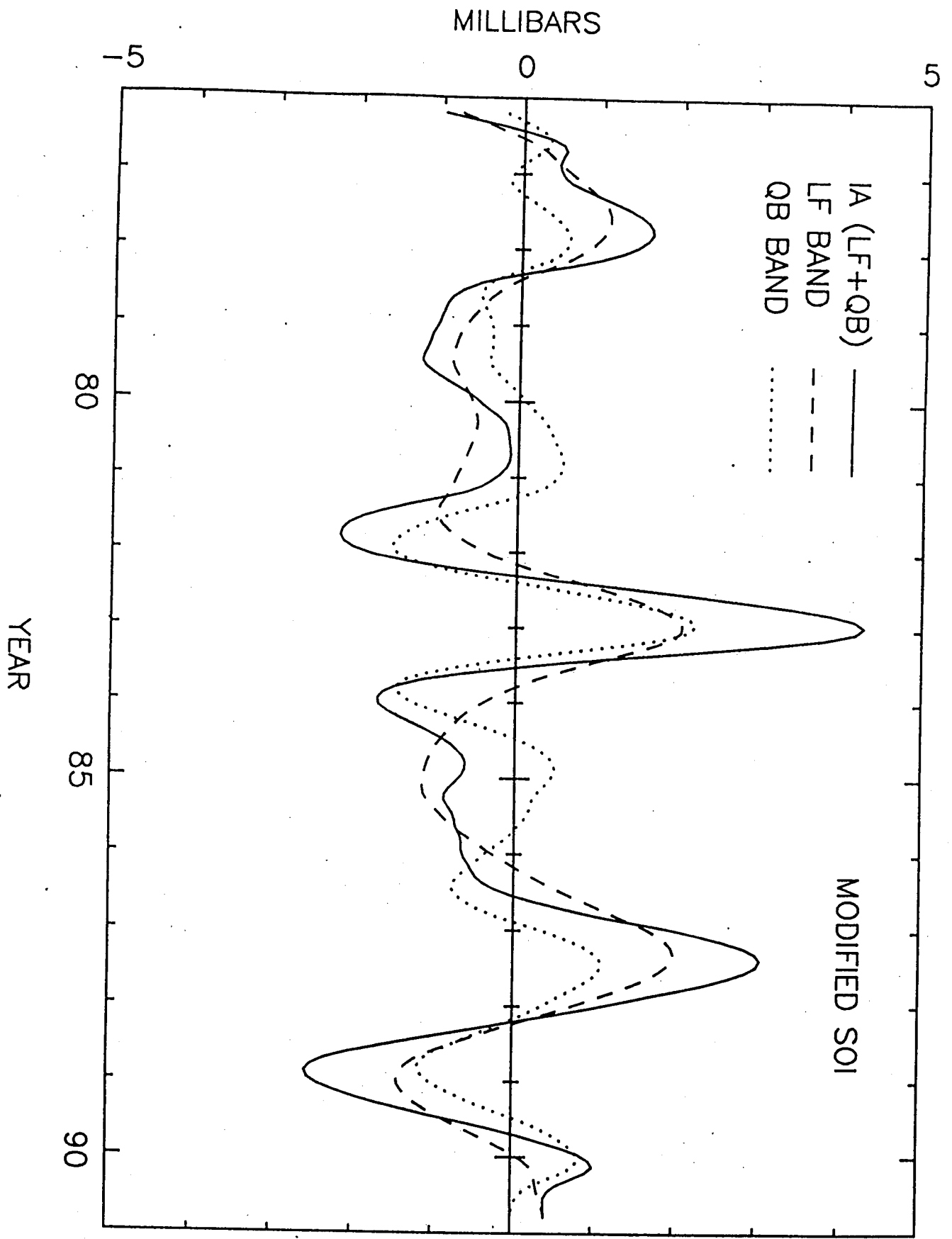


Fig 2b

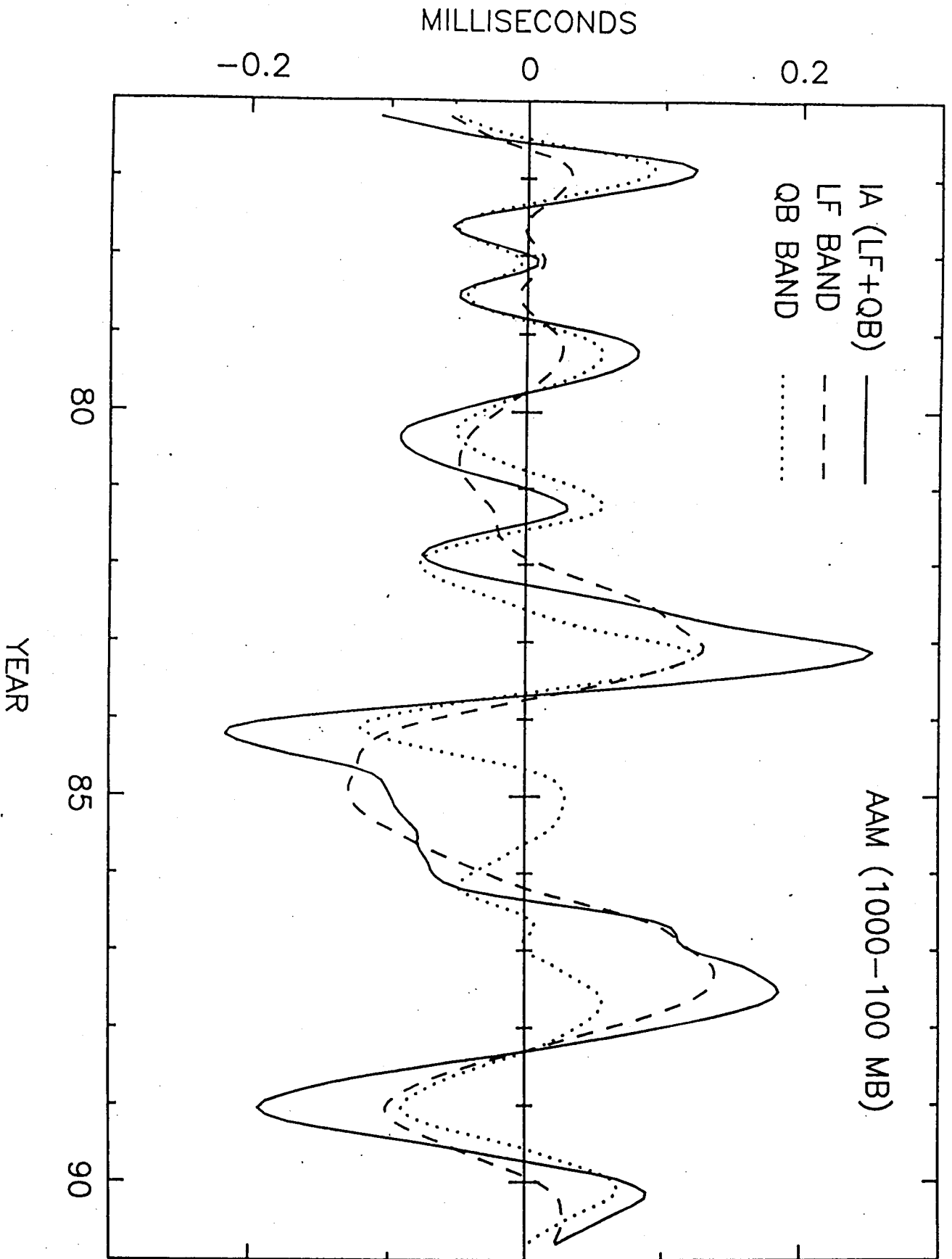


Fig 2a

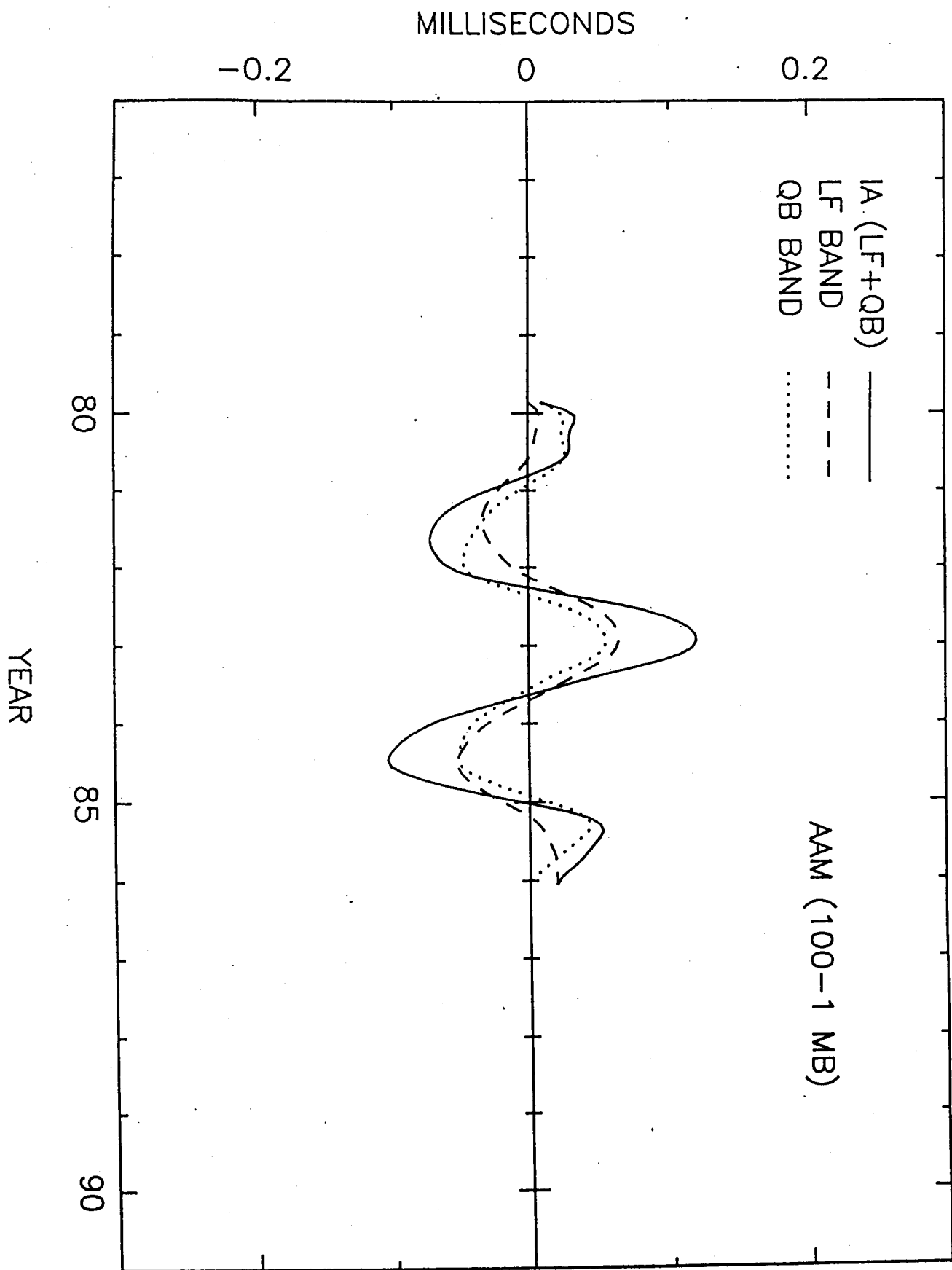


Fig 2a

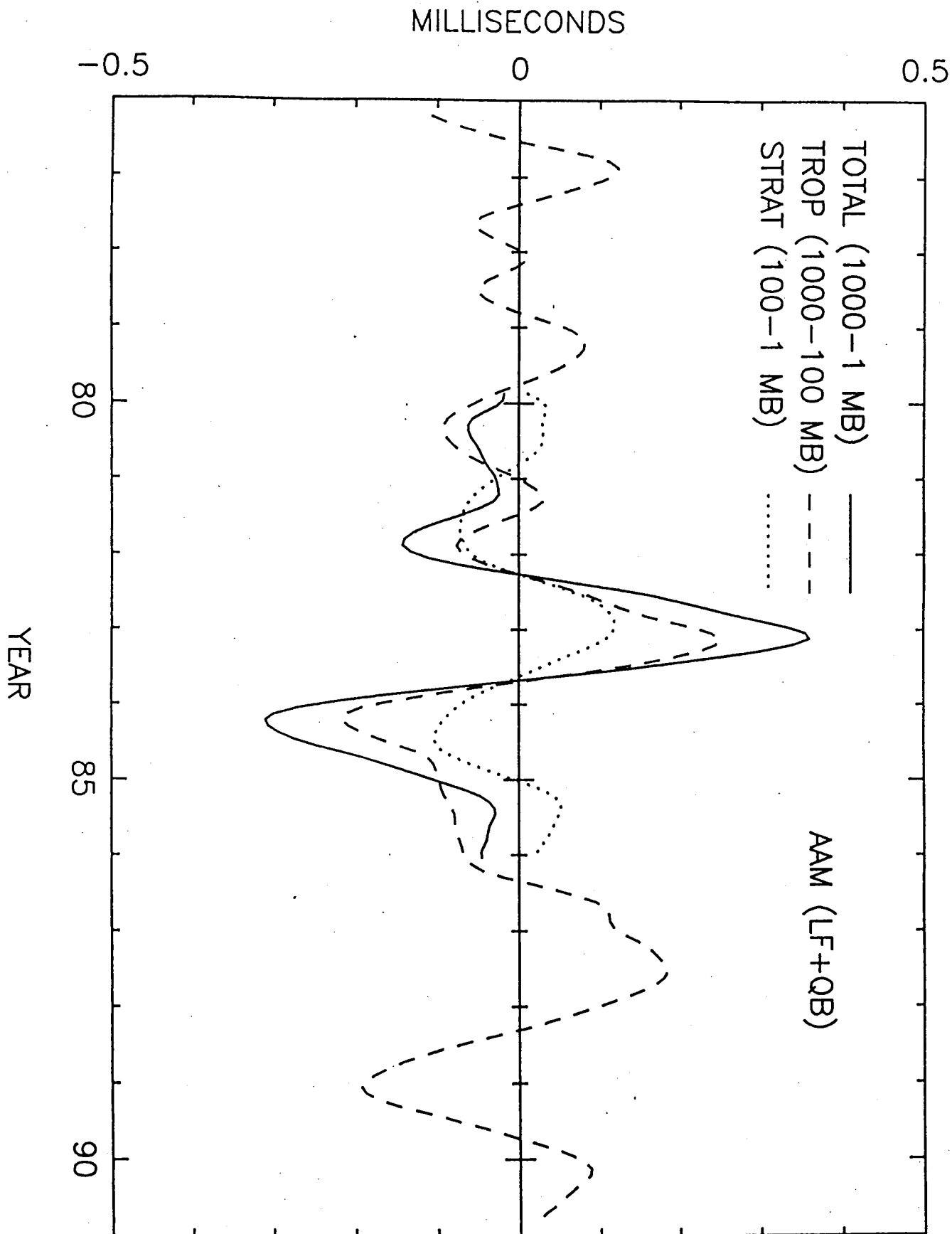


Fig 7e